



Review

Biogenic Synthesis of Copper-Based Nanomaterials Using Plant Extracts and Their Applications: Current and Future Directions

Jei Vincent ¹, Kam Sheng Lau ^{1,*}, Yang Chia-Yan Evyan ², Siew Xian Chin ³, Mika Sillanpää ^{1,4,5,6} and Chin Hua Chia ^{1,*}

- ¹ Materials Science Program, Department of Applied Physics, Faculty of Science and Technology, Universiti Kebangsaan Malaysia, Bangi 43600, Selangor, Malaysia
- ² Faculty of Engineering, Science and Technology, Nilai University, Nilai 71800, Negeri Sembilan, Malaysia
- ³ ASASpintar Program, Pusat GENIUS@Pintar Negara, Universiti Kebangsaan Malaysia, Bangi 43600, Selangor, Malaysia
- ⁴ Department of Chemical Engineering, School of Mining, Metallurgy and Chemical Engineering, University of Johannesburg, P.O. Box 17011, Doornfontein 2028, South Africa
- ⁵ Sustainable Membrane Technology Research Group (SMTRG), Chemical Engineering Department, Persian Gulf University, Bushehr P.O. Box 75169-13817, Iran
- ⁶ Zhejiang Rongsheng Environmental Protection Paper Co., Ltd., NO. 588 East Zhennan Road, Pinghu Economic Development Zone, Zhejiang 314213, China
- * Correspondence: lauks@ukm.edu.my (K.S.L.); chia@ukm.edu.my (C.H.C.)

Abstract: Plants have been used for multiple purposes over thousands of years in various applications such as traditional Chinese medicine and Ayurveda. More recently, the special properties of phytochemicals within plant extracts have spurred researchers to pursue interdisciplinary studies uniting nanotechnology and biotechnology. Plant-mediated green synthesis of nanomaterials utilises the phytochemicals in plant extracts to produce nanomaterials. Previous publications have demonstrated that diverse types of nanomaterials can be produced from extracts of numerous plant components. This review aims to cover in detail the use of plant extracts to produce copper (Cu)-based nanomaterials, along with their robust applications. The working principles of plant-mediated Cu-based nanomaterials in biomedical and environmental applications are also addressed. In addition, it discusses potential biotechnological solutions and new applications and research directions concerning plant-mediated Cu-based nanomaterials that are yet to be discovered so as to realise the full potential of the plant-mediated green synthesis of nanomaterials in industrial-scale production and wider applications. This review provides readers with comprehensive information, guidance, and future research directions concerning: (1) plant extraction, (2) plant-mediated synthesis of Cu-based nanomaterials, (3) the applications of plant-mediated Cu-based nanomaterials in biomedical and environmental remediation, and (4) future research directions in this area.

Keywords: biogenic synthesis; copper-based nanomaterials; extraction method; plant extract



Citation: Vincent, J.; Lau, K.S.; Evyan, Y.C.-Y.; Chin, S.X.; Sillanpää, M.; Chia, C.H. Biogenic Synthesis of Copper-Based Nanomaterials Using Plant Extracts and Their Applications: Current and Future Directions. *Nanomaterials* **2022**, *12*, 3312. <https://doi.org/10.3390/nano12193312>

Academic Editor: Sotirios Baskoutas

Received: 6 September 2022

Accepted: 19 September 2022

Published: 23 September 2022

Publisher's Note: MDPI stays neutral with regard to jurisdictional claims in published maps and institutional affiliations.



Copyright: © 2022 by the authors. Licensee MDPI, Basel, Switzerland. This article is an open access article distributed under the terms and conditions of the Creative Commons Attribution (CC BY) license (<https://creativecommons.org/licenses/by/4.0/>).

1. Introduction

Apart from food, plants have traditionally been used intensively in textile, cosmetics, and medicine. Beyond traditional Chinese medicine and Ayurveda, which have developed over thousands of years of interest in the prevention and treatment of diseases, the biomedical applications of plants have broadened even further due to the advancement of technology and of time [1–4]. These biomedical applications are mainly due to the phytochemicals within plants [5–7], which are among the most fascinating aspects of plants due to their having activities such as antimicrobial, antitumour, antiaging, and others [8]. Awareness of such properties has driven researchers to discover still more applications of phytochemicals. In 1959, Richard Feynman illustrated the controlling of single atoms and molecules under the topic of “There’s plenty of room at the bottom”, which first shed light

on the novel nanotechnology research field. More recently, an innovative interdisciplinary study pioneered nanomaterial synthesis from the phytochemicals within plant extracts, a process which is more eco-friendly than conventional methods and avoids the usage of hazardous chemicals [9,10].

Plant-mediated nanomaterials synthesis is a branch of green synthesis in which the phytochemical compounds in plant extracts are utilised as stabilizing and reducing agents [9–13]. In addition to the pros and cons inherent in the synthesis method, the choice of method and parameters in the nanomaterial production process also affect the geometry of the obtained nanomaterials [14]. Typically, plant-mediated synthesis uses a bottom-up approach for material synthesis from plant extracts with the assistance of different biotechnological methods [11,13,15,16]. Conventional synthesis techniques have their disadvantages, such as use of hazardous chemicals, biological risks, and high energy consumption [11,13,17–20]. Relative to conventional approaches like physical and chemical synthesis routes, plant synthesis is considered more eco-friendly and less toxic [13].

Many researchers have successfully synthesised, via plant-mediated synthesis, various types of nanomaterials that were previously produced by conventional synthesis approaches, such as alloys, pure metals, metal oxides, and core shells [21–28]. The produced nanomaterials have been used for numerous applications, including as antibacterials, anti-cancer agents, antifungals, antiparasitics, antioxidants, catalytic reduction agents, catalysts, biosensors, drug delivery vehicles, fuel cells, photocatalysts, and theranostics [24,29–35]. However, there remain some limitations to the plant-mediated synthesis method that need to be addressed, such as the complexity and diversity of phytochemicals in plant systems, bio-reduction reactions, homogeneity, scaling-up, reproducibility, material accessibility, and product stability [31,36].

Cu is an element that has drawn significant attention from researchers in nanotechnology, specifically in the nanomaterial sector [37]. This is owing to the low cost, good abundance, and conductivity exhibited by Cu as compared to silver (Ag) and gold (Au) [38–43]. Accordingly, not only have various Cu nanomaterials (Cu-NMs) been developed, but there is a good body of literature on the plant-mediated synthesis of Cu nanomaterials with various applications [11].

Therefore, this review will focus on the synthesis of Cu-NMs from several perspectives, including their conventional, green, and especially plant-mediated synthesis, and, relatedly, plant extraction methods, parameters of plant-mediated nanomaterials, applications of plant-mediated Cu-NMs, limitations of plant-based synthesis and proposed solutions, and potential new applications and new research directions that are yet to be explored regarding plant-mediated Cu-NMs.

2. Synthesis of Nanomaterials: Conventional and Green Approaches

Approaches for the production of nanomaterials can be categorised according to two predominant aspects: top-down and bottom-up [44]. Examples of the subdivisions within each sector will be discussed. Firstly, top-down nanomaterial synthesis methods composed of ball milling and laser ablation, then bottom-up methods including hydrothermal, vapor deposition, microwave, chemical reduction, and green synthesis [45,46].

2.1. Disadvantages of Conventional Nanomaterial Synthesis Method

The typical demerits of conventional methods can be observed clearly in the case of ball milling, as it is both energy-intensive and time-consuming to produce nanomaterials by this method, and, hence, ball milling is neither economical nor industry-friendly [45–47]. Similarly, the other top-down approach, laser ablation, requires high energy input to produce a sufficiently intense laser for the continuous ablation process [46,48]. On the other hand, among bottom-up approaches, hydrothermal and microwave methods require an expensive autoclave and complex equipment; thus, they are not applicable economically [45,46,48,49], while vapor deposition also necessitates high energy consumption [50]. Meanwhile, chemical reduction utilises many substances that exhibit high toxicity toward living organisms and the environment, such as hydrazine, N, N-dimethylformamide, and sodium borohy-

dride; this results in additional treatment processes also being required [51,52]. Given all of the above drawbacks, many researchers have investigated green synthesis methods in order to discover more biologically friendly alternatives for producing nanomaterials.

2.2. Green Synthesis Method of Nanomaterials

Green synthesis methods that utilise natural or biological compounds to produce nanomaterials, such as bacterial-, fungal-, algae-, and plant-based methods, have been found to be non-toxic, non-harmful, and eco-friendly [14,37,47]. The utilization of natural and biologically friendly compounds as reducing or capping agents also offers other advantages such as reducing energy requirements, avoiding usage of toxic/hazardous chemicals, and being simple and cheap [11,13,53]. The synthesis of nanomaterials using bacteria has particular advantages as bacteria is abundant, easily cultured with a short generation time, inexpensive to cultivate, stable, and easy to manipulate at the genetic level [46,54]. On top of that, previous reports have described the adaptability of bacteria to environments with a high concentration of heavy metals via transforming the toxic metal ions to non-toxic metal oxide nanomaterials, which provides another rationale for the utilization of bacteria in nanomaterial production, as precursors could be introduced in higher concentrations [55,56].

In the fungal-mediated synthesis of nanomaterials, fungi show outstanding heavy-metal tolerance, internalization, and bioaccumulation capability, making them good candidates as reducing and stabilizing agents in the synthesis of metal nanomaterials [57]. Moreover, fungi can be reproduced in large quantities, and by the parity of reasoning nanomaterials can be synthesised in quantity [58]. Relative to bacteria, fungi produce higher amounts of proteins and enzymes; thus, they can provide higher productivity of synthesis [46,59].

Algal-mediated synthesis of nanomaterials involves the utilization of carbohydrates, proteins, minerals, lipids, and bioactive compounds within algae as reducing agents to reduce metal precursor ions into nanomaterials [60]. Given their heavy-metal hyperaccumulation capability, algae are excellent candidates for nanomaterials synthesis [61,62]. The algae-mediated production of nanomaterials can occur either via extracellular or intracellular processes and affords good control over production parameters [60]. However, although the various microorganism-mediated synthesis processes offer many benefits, the pathogenic properties of organisms, underlying safety concerns, and deficit of knowledge regarding synthesis mechanisms are drawbacks that yet hinder the use of these processes in industrial nanomaterial production and applications [46,54,63].

Plants are particularly good candidates for nanomaterial synthesis since they have no pathogenic effects as microorganisms do, plus the nanomaterials produced via plant biogenic synthesis are more homogenous in comparison to the products of other methods [46,54]. In addition, unlike other synthesis methods, the mechanism of plant-mediated metal nanoparticle synthesis is limited to the reduction of a precursor salt via agents within the plant extract in the presence of a metal ion precursor. Moreover, stabilizing agents within a plant extract can also attach to the surface of the produced nanoparticles, improving the surface reaction kinetics as well as particle stability and, hence, reducing the deformation and agglomeration of particles [64]. The reducing and stabilizing agents that participate in the formation of nanomaterials consist of phytochemicals such as amino acids, proteins, vitamins, terpenes, flavones, ketones, amides, saponins, phenolics, terpenoids, aldehydes, alkaloids, carboxylic acids, and polysaccharides naturally found within the plant [11,13].

3. Plant-Mediated Nanomaterial Synthesis

The most essential element in plant-mediated nanomaterial synthesis is the plant extract. While a number of approaches have been developed for obtaining extracts, the overall technique can be generalised into the few steps illustrated in Figure 1.

Notably, extracts can be obtained from multiple different parts of plants, including leaves, fruits, peelings, flowers, rhizomes, roots, and seeds; see Table 1.

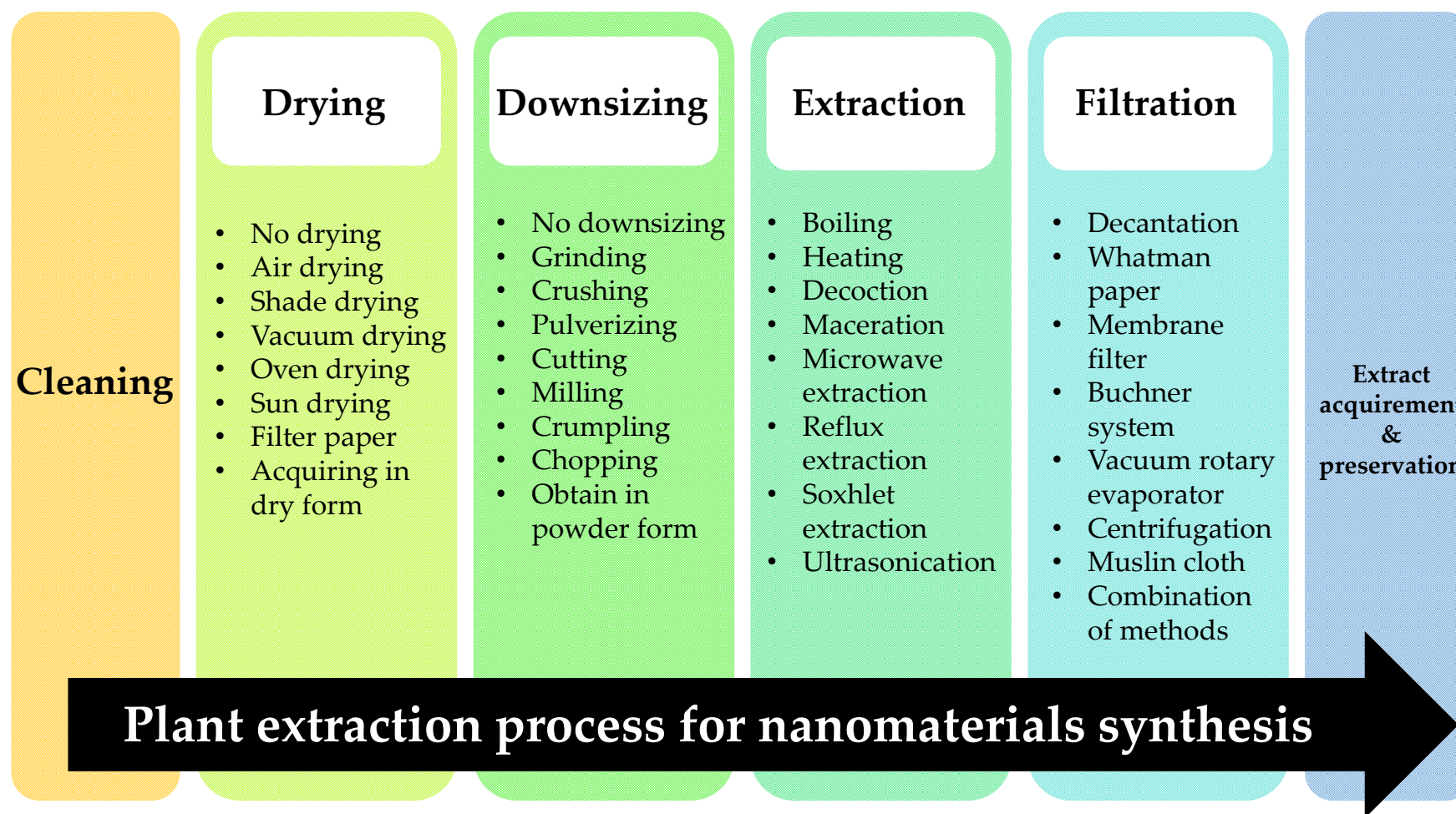


Figure 1. General steps in plant extraction.

Table 1. Parameters and extraction method utilised for extraction of different plant components.

Species	Drying	Downsizing Method	Extraction Method	Temperature (°C)/Power	Time	Solvent	Reference
Leaves							
<i>Azadirachta indica</i>	Oven drying at 50 °C	-	Heating	60	20 min	DI-H ₂ O	[65]
<i>Basella alba</i>	Shade drying at room temperature	Grinding and pulverizing	Boiling	60	20 min	DI-H ₂ O	[66]
<i>Cacumen platycladi</i>	Acquired in dried form	Milling	Heating	30	4 h	DI-H ₂ O	[67]
<i>Carica papaya</i>	Shade drying	Grinding	Boiling	60	30 min	DI-H ₂ O	[68]
<i>Cymbopogon jwarancusa</i>	Shade drying at room temperature	Grinding	Boiling	Step 1: 100 Step 2: 37	Step 1: 30 min Step 2: overnight	Double DS-H ₂ O	[69]
<i>Daphne mezereum</i>	Acquired in dried form	Acquired in cut form	Reflux extraction	-	15 min	DI-H ₂ O	[70]
<i>Eclipta prostrata</i>	-	-	Boiling	80	30 min	Double DS-H ₂ O	[71]
<i>Ixora brachypoda</i>	Air drying at room temperature	Cutting	Boiling	60	1 h	DI-H ₂ O	[72]
<i>Iresine herbstii</i>	Drying	Pulverizing	Soxhlet extraction	-	12–16 h	Ethanol	[73]
<i>Jasminum sambac</i>	-	Cutting	Microwave irradiation	-	200 s	DS-H ₂ O	[74]
<i>Magnolia kobus</i>	Drying at room temperature	Cutting	Boiling	-	5 min	DS-H ₂ O	[75]
<i>Menthaaquatica</i>	Drying	Grinding	Ultrasonication	400 W	10 min (On/Off = 7 s/3 s)	DI-H ₂ O	[76]
<i>Moringa oleifera</i>	Drying at room temperature	Grinding	Soxhlet extraction	35–45	10 h	Methanol	[77]
<i>Piper betle</i>	Shade drying at room temperature	Cutting	Boiling	-	5 min	Double-distilled deionised water	[78]
<i>Plantago asiatica</i>	Acquired in dried form	Acquired in powder form	Reflux extraction	80	30 min	Double DS-H ₂ O	[79]
<i>Quercus coccifera</i>	Drying at room temperature	Grinding	Boiling	90	30 min	DS-H ₂ O	[80]
<i>Ruellia tuberosa</i>	-	Chopping	Boiling	50	10 min	DI-H ₂ O	[81]
<i>Solidago canadensis</i>	Drying at room temperature	Grinding	Heating	80	-	DS-H ₂ O	[82]
<i>Syzygium cumini</i>	Oven drying at 60 °C	Crumpling	Boiling	100	35 min	DI-H ₂ O	[83]
<i>Tabernaemontana divaricate</i>	-	Grinding	Boiling	-	10 min	DI-H ₂ O	[84]
<i>Thymus vulgaris</i>	Acquired in dried form	Grinding	Reflux extraction	70	2 h	DS-H ₂ O	[85]
<i>Tradescantia spathacea</i>	-	Chopping	Boiling	60	60 min	DI-H ₂ O	[86]
<i>Camellia sinensis</i>							
<i>Citrus limon</i>							
<i>Eucalyptus globulus</i>							
<i>Laurus nobilis</i>							
<i>Mentha sp.</i>							
<i>Quercus robur</i>	Acquired in dried form	-	Reflux extraction	-	40 min	DI-H ₂ O	[87]
<i>Rosmarinus officinalis</i>							
<i>Thimus mastichina</i>							
<i>Thimus vulgaris</i>							
<i>Thuja occidentalis</i>							
Fruits							
<i>Berberis vulgaris</i>	Acquired in dry form	Acquired in powder form	Heating	80	30 min	Double DS-H ₂ O	[88]
<i>Capparis spinosa</i>	Oven drying (12 h) (383 K)	-	Boiling	-	30 min	Ethanol/ H ₂ O (ratio-1:1)	[89]
<i>Citrus medica</i>	-	-	Squeezing to get juice	-	-	-	[51]
<i>Citrus sinensis</i>	-	Cutting	Squeezing to get juice	-	-	-	[90]
<i>Cleome viscosa</i>	-	-	Boiling	60	30 min	DS-H ₂ O	[91]
<i>Couroupita guianensis</i>	Shade drying for 8–10 days	Chopping, grinding	Decoction	60	20 min	DS-H ₂ O	[92]
<i>Crataegus pentagyna</i>	-	-	Maceration	-	-	Methanol	[93]
<i>Emblcia officinalis</i>	-	Crushing	Boiling	-	10 min	Double DS-H ₂ O	[94]

Table 1. Cont.

Species	Drying	Downsizing Method	Extraction Method	Temperature (°C)/Power	Time	Solvent	Reference
Leaves							
<i>Ficus carica</i>	Acquired in dry form	Chopping	Heating	100	1 h	Double DS-H ₂ O	[95]
<i>Lycium barbarum</i>	-	-	Boiling	-	8 min	DI-H ₂ O	[96]
<i>Piper longum</i>	Acquired in dry form	Acquired in powder form	Heating	70	30 min	30% methanolic solution	[97]
<i>Pouteria caimito</i>	Shade drying at room temperature	Cutting	Steeping	-	-	DS-H ₂ O	[98]
<i>Sechium edule</i>	-	-	Heating	90 ± 2	12 h	DS-H ₂ O	[99]
<i>Solanum mammosum</i>	Oven drying (25 °C)	Grinding	Mixing with solvent/maceration	-	1 h	DI-H ₂ O	[100]
<i>Syzygium alternifolium</i>	Acquired in dry form	Acquired in powder form	Boiling	80	30 min	Milli-Q water	[101]
<i>Vaccinium macrocarpon</i>	Acquired in dry form	Grinding	Reflux extraction	90	45 min	DS-H ₂ O	[102]
Peelings							
<i>Allium cepa</i>	Acquired in dry form	Cutting	Heating	90	30 min	DS-H ₂ O	[103]
<i>Annona squamosa</i>	Air-drying	Grinding	Heating	60	30 min	Double DS-H ₂ O	[104]
<i>Arachis hypogaea</i>	Oven drying method for 70 °C for 30 min	Peeling via oven drying method	Heating	70	30 min	Water	[105]
<i>Benincasa hispida</i>	-	-	Boiling	-	30 min	DS-H ₂ O	[106]
<i>Carica papaya</i>	-	Acquired in small pieces	Heating	70–80	20 min	DI-H ₂ O	[26]
<i>Citrus sinensis</i>	-	Smashing and grinding	Mixing	-	4 h	DI-H ₂ O	[107]
<i>Garcinia mangostana</i>	Drying at ambient conditions; later with crude extract via oven drying	Grinding	Heating	80	1 h	Double DI-H ₂ O	[108]
<i>Garcinia mangostana</i>	Oven drying at 40 °C	Grinding	Boiling	60	30 min	DS-H ₂ O	[109]
<i>Myristica fragrans</i>	Acquired in dry form	Acquired in ground form	Boiling	100	1 h	DI-H ₂ O	[110]
Orange peel	Drying by food drier for 12 h	Peeling and grinding	Stage 1: Maceration Stage 2: Heating	Stage 1: none Stage 2: 60	Stage 1: 3 h Stage 2: 60 min	DI-H ₂ O	[111]
<i>Persea americana</i>	-	Milling	Maceration	-	24 h	DS-H ₂ O	[112]
<i>Punica granatum</i>	Air-drying under shade	Chopping and grinding	Soxhlet extraction	55	30 min	DI-H ₂ O	[113]
<i>Punica granatum</i>	Shade drying	-	Boiling	-	10 min	DS-H ₂ O	[114]
<i>Punica granatum</i>	Oven drying 60 °C for 40 h	Acquired in powder form	Mixing	-	24 h	100% Ethanol	[115]
Tangerine	Shade drying (27 ± 2 °C)	Milling by electric mill and sieving	Heating	80	15 min	DS-H ₂ O	[116]
<i>Citrus aurantifolia</i>	-	-	Stage 1: Maceration with solvent Stage 2: Heating	Stage 1: none Stage 2: 60	Stage 1: 3 h Stage 2: 60 min	DI-H ₂ O	[117]
<i>Citrus paradisi</i>	Drying via food dryer	Grinding	-	-	-	-	-
<i>Citrus sinensis</i>	-	-	-	-	-	-	-
<i>Lycopersicon esculentum</i>	-	-	-	-	-	-	-
Flowers							
<i>Aglaia elaeagnoides</i>	Shade drying for 3 days	Grinding	Reflux extraction	-	10 min	DI-H ₂ O	[118]
<i>Achillea wilhelmsii</i>	Air drying	Cutting	Boiling	-	10 min	Sterile DS-H ₂ O	[119]
<i>Aloe vera</i>	Oven drying at 50 °C for 72 h	Cutting	Boiling	-	5 min	Double DS-H ₂ O	[120]
<i>Avicennia marina</i>	-	Grinding	Boiling	-	5 min	DS-H ₂ O	[121]
<i>Azadirachta indica</i>	Shade drying for a week	Crushing	Heating	80	1 h	DI-H ₂ O	[122]
<i>Calendula</i>	Drying at room temperature	-	Heating	80	30 min	DI-H ₂ O	[123]
<i>Gazania rigens</i>	Shade drying with oven drying	Cutting and grinding	-	-	3 h	Methanol	[124]
<i>Gnidia glauca</i>	Shade drying for 2 days at room temperature	Grinding	Boiling	-	5 min	DS-H ₂ O	[125]

Table 1. Cont.

Species	Drying	Downsizing Method	Extraction Method	Temperature (°C)/Power	Time	Solvent	Reference
Leaves							
<i>Hibiscus sabdariffa</i>	Air drying under shade at room temperature		Soaking	Room temperature	2 h	DS-H ₂ O	[126]
<i>Muntingia calabura</i>	-	-	Boiling via microwave oven	-	Boiling: 1 min * Process repeated at 1 h intervals for up to 6 h	DS-H ₂ O	[127]
<i>Tagetes erecta</i>	-	Cutting	Boiling	-	10 min	Ultra-pure water	[128]
<i>Trifolium pratense</i>	Air drying for 5 days at room temperature	-	Heating	80	45 min	Double DS-H ₂ O	[129]
Roots and Rhizomes							
<i>Berberis vulgaris</i>	Drying at ambient temperature for 2 days	Grinding	-	Room temperature	2 days	Sterile DS-H ₂ O	[130]
<i>Bergenia ciliata</i>	Air drying at 25 °C	Acquired in powder form	Boiling	60	30 min	Milli-Q water	[131]
<i>Chromolaena odorata</i>	Sun drying At 22 °C ± 2 °C for 14 days	Crushing	Heating	85	2 h	DI-H ₂ O	[132]
<i>Cibotium barometz</i>	Drying	Cutting and pulverizing	Boiling	100	30 min	DS-H ₂ O	[133]
<i>Diospyros paniculata</i>	Air drying	Grinding	Soxhlet extraction	-	-	Methanol	[134]
Licorice	-	-	Heating	-	-	Ethanol and double-ionised water	[135]
<i>Morinda citrifolia</i>	Shade drying at room temperature	Grinding	Boiling	-	15 min	DS-H ₂ O	[136]
<i>Nepeta leucophylla</i>	Shade drying for 30 days at room temperature (24–32 °C)	Grinding	Soxhlet extraction	Boiling point of methanol	8 h	Methanol	[137]
<i>Panax ginseng</i>	-	Cutting and grinding	Boiling	-	30 min	Sterile water	[138]
<i>Rheum palmatum</i>	Acquired in dry form	Acquired in powder form	Reflux extraction	80	45 min	Ethanol	[139]
<i>Rheum palmatum</i>	-	Acquired in powder form	Incubating/heating	40	24 h	Milli-Q DI-H ₂ O	[140]
<i>Rhodiola rosea</i>	-	Grinding and screening via sieve	Boiling	100	30 min	DI-H ₂ O	[141]
<i>Scutellaria baicalensis</i>	Acquired in dry form	Grinding	Autoclave heating	100	30 min	DS-H ₂ O	[142]
<i>Zingiber officinale</i>	-	Grinding	Microwave	-	1 min	DI-H ₂ O	[143]
<i>Zingiber officinale</i>	-	Cutting and pulverizing	Squeezing	-	-	-	[144]
Seeds							
<i>Bixa orellana</i>	Vacuum drying at 60 °C	Crushing	Steeping	In dark environment	24 h	Ethanol	[145]
<i>Caesalpinia bonducella</i>	-	Grinding	Sonication	-	30 min	DI-H ₂ O	[146]
<i>Coffea arabica</i>	-	Grinding	Heating	85	25 min	DS-H ₂ O	[147]
<i>Cucurbita pepo</i>	Shade air drying for 2 days	-	Heating	90	2 h	DS-H ₂ O	[148]
<i>Eriobotrya japonica</i>	Oven drying at 50 °C for 24 h	Grinding	Heating	40	60 min	DI-H ₂ O	[149]
<i>Persea americana</i>	Drying in dryer for 12 h	Grinding	-	Stage 1—room temperature Stage 2—65 ± 1	Stage 1: 60 min Stage 2: 60 min	DI-H ₂ O	[150]
<i>Phoenix dactylifera</i>	-	Milling	Boiling	80	20 min	Sterile DS-H ₂ O	[151]
<i>Phoenix sylvestris</i>	-	-	Steeping	45	12 h	Sterile double DI-H ₂ O	[152]
Pomegranate	-	-	Crushing to get juice	-	-	DI-H ₂ O	[153]
<i>Punica granatum</i>	Drying by pressing in filter paper	Grinding	Heating	80–85	10 min	Ultra-pure water	[154]
<i>Punica granatum</i>	-	Grinding	Mixing	-	2 h	Water	[155]

Table 1. Cont.

Species	Drying	Downsizing Method	Extraction Method	Temperature (°C)/Power	Time	Solvent	Reference
Leaves							
Quince	-	-	Heating	60	4 h	DS-H ₂ O	[156]
<i>Salvia hispanica</i>	Drying	-	Heating	60	120 min	DS-H ₂ O	[157]
<i>Tectona grandis</i>	Drying at room temperature for 3–4 days	Crushing	Boiling	80	15–20 min	Double DS-H ₂ O	[158]
<i>Theobroma cacao</i>	Drying at room temperature for a week	Grinding	Maceration	-	A week	Methanol	[159]

3.1. Plant Extraction Method

The first step of plant extraction is the cleaning process, which mainly aims to remove debris or dust with water so as to avoid any form of contamination that might affect the subsequent synthesis process. The second step consists of drying and downsizing. Drying is necessary to avoid the deterioration of phytochemicals that results from enzymatic and microbial activities due to the presence of water moisture [160].

3.1.1. Drying

Typically, drying is performed via air drying, shade drying, oven drying, drying in a dehydrator, vacuum drying, sun drying, or on filter paper; plant materials can also be acquired in the dry form (Table 1 and Figure 1).

Each of the abovementioned drying methods is able to successfully yield plant extracts with phytochemicals. Shade and air drying are considered among the best methods as they allow the greatest preservation of nutrients, such as proximate and ascorbic acid, and do so with lower financial cost as compared to mechanical drying methods such as oven drying, vacuum drying, or using a food dryer [160]. As a case in point, tangerine peel was shade dried at 27 ± 2 °C for the synthesis of iron oxide nanoparticles [116]. However, due to being carried out at a lower temperature, shade and air drying require a longer period of time than other drying methods, which might reduce their applicability in the industrial plant-mediated synthesis of Cu-NMs [160]. For instance, in preparation for Au nanoparticle synthesis, *Nepeta leucophylla* root was shade dried at room temperature (24–32 °C) for 30 days [137]. Sun drying was also used in drying *Chromolaena odorata* for the synthesis of Fe₃O₄ nanoparticles from phenolic components of the extract [132]. While sun drying can reduce the cost of drying just as can shade drying, it is not recommended for industrial synthesis due to high labour demand, low efficiency, hygiene issues, and more precautions being required to avoid contamination of samples [160].

The temperature of the drying process also plays a major role in preserving the phytochemicals within a plant. Specifically, drying temperatures in the range of 40–60 °C are reported to support the minimal loss of phytochemicals in plant components [160]. In prior studies, neem leaves (*Azadirachta indica*) were oven dried for 15 min at 50 °C [65], and *Garcinia mangostana* peelings for 10 min at 40 °C [109]. Although the range of 40–60 °C is recommended, the final decision on which temperature is most suitable for the drying process should be based on the characteristics of the plant material being dried. For example, a study oven dried *Arachis hypogaea* at 70 °C for 30 min due to its anthocyanin content, which is highly preserved under those drying parameters [105]. Nonetheless, drying at room/ambient temperature remains the most used method owing to the low cost requirement being beneficial to industrialization. For instance, Irum et al. [69] shade dried *C. jwarancusa* at room temperature while Elgorban et al. [123] dried calendula flowers at room temperature to acquire phytochemicals. This is despite the time requirement being much higher; for instance, when drying at room temperature, Yulizar et al. [159] took a week to dry *Theobroma cacao* seeds and Rautela et al. [158] 3–4 days for *Tectona grandis* seeds in preparation for nanoparticle synthesis. On the other hand, Pan et al. [105] only need 30 min to dry *Arachis hypogaea* with an oven at 70 °C in plant-mediated iron nanoparticle synthesis, while Doan Thi et al. [111] took 12 h to dry orange peels for ZnO nanoparticle production.

In addition to the abovementioned drying methods, some plant components simply are not subjected to any drying process, mainly in the interest of cost saving and because certain components have high water contents that will increase the cost if a drying process is applied. Such plant components can include fruits, flowers, seeds, roots, and rhizomes. In one example, Jahan et al. [90] squeezed the juice from *Citrus sinensis* fruits to acquire reducing sugars, amino acids, proteins, and metabolites such as flavanones and terpenoids for the synthesis of Cu nanoparticles. The same squeezing method was also applied to *Zingiber officinale* root by Velmurugan et al. [144] to acquire alkaloids and flavonoids for the synthesis of Au and Au nanoparticle. Crushing is another technique for acquiring plant extracts; for example, Kumari et al. [153] crushed pomegranate seeds to obtain flavonoids and terpenoids for the synthesis of Au-Ag bimetallic nanoparticles. Moreover, some methods forgo any drying treatment, such as when Patra et al. [127] directly extracted *Muntingia calabura* flowers to acquire phytochemicals for nanoparticle synthesis and

Al-Radadi [135] used licorice root without drying to obtain glycosides, organic acids, phenolic compounds, and flavonoids for the synthesis of Au nanoparticles. Ultimately, the characteristics of the plant component being used and the potential cost are important factors informing the best drying method and parameters by which to obtain the most phytochemicals from plant components for Cu-NM synthesis for either research or industrial purposes.

3.1.2. Downsizing

Regarding the downsizing step, its primary purpose is to reduce the size of the plant components and increase their surface area, leading to better diffusivity and mass transfer in order to extract the greatest yields of phytochemicals such as polyphenolic compounds, phenolic acids, and tannins [161]. There are various routes for achieving this objective, presented in Table 1 and Figure 1. Interestingly, miniscule deviations of plant component size can cause significant alterations in overall phytochemical yield [161]. Therefore, it is necessary to consider carefully the most suitable methods and cost requirements so as to acquire the smallest plant components with the highest phytochemical yields for Cu-NM synthesis. Just as with the drying process, there are some plant components that do not undergo any downsizing, such as those with high water content; for example, *Crataegus pentagyna* fruits were extracted by Ebrahimpzadeh et al. [93] without any downsizing.

3.1.3. Plant Extraction Methods

Plant extraction methods are mainly based on boiling and heating (Table 1). Mani et al. [66] conducted an extraction from dried, ground, and pulverised *Basella alba* leaves by mixing them with DI-H₂O and boiling them in a water bath at 60 °C for 20 min. Nnadozie and Ajibade [132] similarly heated crushed *Chromolaena odorata* at 85 °C for 2 h in DI-H₂O, and Abisharani et al. [148] heated *Cucurbita pepo* seeds with DS-H₂O at 90 °C for 2 h.

Interestingly, some alternative methods have been introduced and successfully used to extract phytochemical products from plants (Table 1). For example, Siddiqui et al. [113] boiled powdered *Punica granatum* peels in sterile DI-H₂O at 55 °C for 30 min on a Soxhlet apparatus, and Singh and Dhaliwal similarly performed Soxhlet extraction on powdered *Nepeta leucophylla* roots with methanol held at boiling for 8 h [137]. Sonication has also been used in plant extractions; for instance, one study removed the coats of *Caesalpinia bonducella* seeds and then sonicated the ground kernels for 30 min [146]. Likewise, reflux extraction has been used with various plant components. Beheshtkhoo et al. [70] extracted *Daphne mezereum* leaves by refluxing the dried leaves with a 5% (*w/v*) mixture in DI-H₂O for 15 min. Microwave irradiation has also been used in extraction, such as in a study that irradiated cut *Jasminum sambac* leaves in DS-H₂O for 200 s to extract phytochemicals for the synthesis of Au, Ag, and Au–Ag alloy nanoparticles [74]. Maceration has also been used by many researchers, mainly due to its low cost and eco-friendliness; for instance, ground *Solanum mammosum* fruits were macerated with DI-H₂O at room temperature and constant agitation for 1 h [100] and *Crataegus pentagyna* fruits with methanol at room temperature for the synthesis of Fe₃O₄-SiO₂-Cu₂O-Ag nanocomposites [93]. In addition to the above, autoclaving was carried out on dried and ground roots of *Scutellaria baicalensis* with DS-H₂O for 30 min at 100 °C in preparation for the synthesis of ZnO nanoparticles [142].

Aside from single extraction methods, combinations of methods have also been applied to acquire extracts from various plants. For example, Nava et al. [117] macerated the peels of *Citrus aurantifolia*, *Citrus paradisi*, *Citrus sinensis* and *Lycopersicon esculentum* for 3 h with stirring, then heated the mixture at 60 °C for 60 min. For plant components with high water content, a squeezing method may be introduced. For example, in the preparation of *Zingiber officinale* root extract by Velmurugan et al. [144], the downsized roots were squeezed via muslin cloth.

Every extraction method has its pros and cons, summarised in Table 2 and Figure 1 [4,161,162]. The most suitable method for any given use case depends on the types of plant components as well as the requirements and restriction posed by the actual environment, such as a need to reduce financial and labour costs for industrial purposes as well as a requirement for eco-friendliness.

Table 2. Pros and cons of various plant extraction methods.

Extraction Methods	Pros	Cons
Boiling/heating/decoction	<ul style="list-style-type: none"> • Water-soluble constituents can be extracted 	<ul style="list-style-type: none"> • Inefficient for light-/heat-sensitive compounds
Maceration	<ul style="list-style-type: none"> • Simple • Low cost and little experimental set-up • Eco-friendly 	<ul style="list-style-type: none"> • Batch-to-batch variation potential • Long extraction time
Microwave extraction	<ul style="list-style-type: none"> • Fast extraction • Less solvent needed • Produce extract with high purity and phenolic yield • Cost effective 	<ul style="list-style-type: none"> • High heat and energy loss during the extraction
Reflux extraction	<ul style="list-style-type: none"> • Less solvent and extraction time required • Good contact efficiency and mass transfer • Simple and easy operation 	<ul style="list-style-type: none"> • Not suitable for thermolabile compounds
Soxhlet extraction	<ul style="list-style-type: none"> • Displacement of transfer equilibrium between plant components and the solvent could be acquired • High extraction temperature could be provided • No filtration requirement after leaching 	<ul style="list-style-type: none"> • Large sample, extraction time, solvent requirements • Excessive loss of heat energy
Ultrasonication	<ul style="list-style-type: none"> • Less residence time of plant particles in the solvent • Lower material and solvent requirements • Fast extraction process 	<ul style="list-style-type: none"> • Energy intensive

Solvents in Plant Extraction

In addition to the extraction method used, solvent, energy consumption, time required, and other parameters are also critical to the extraction of phytochemicals [161,163,164]. Extraction solvents can be divided into two types. i.e., water (distilled, double distilled, Milli-Q, ultra-pure, and deionised) and alcoholic solvents (ethanol and methanol), as presented in Table 1. Water (DS-H₂O) was used to extract dried and ground *Quercus coccifera* leaves with boiling for 30 min at 90 °C [80]. Conversely, Boruah et al. [77] produced *Moringa oleifera* leaf extract by Soxhlet extraction with methanol as the solvent, incubating the dried and powdered leaves at 35–45 °C for 10 h. Some phytochemicals, such as polyphenolic compounds, anthocyanins, and polyphenols, can be obtained at higher yields when an alcoholic solvent is involved. Conversely, Do et al. [165] found that the phytochemical extraction yield from *Limnophila aromatica* improves as the solvent polarity increases; in particular, methanol could extract more phytochemicals than ethanol. There are also some cases that benefit from extraction solvents combining both water and an alcoholic solvent. For example, *Piper longum* fruits were dried, powdered and extracted with 30% methanolic solution at 70 °C for 30 min [97], and Zarei et al. [89] used ethanol and water at a 1:1 ratio with boiling for 30 min. Remarkably, such combinations of alcoholic solvents with water can achieve the highest yields due to allowing for greater solubility of plant components [161,165,166]. Therefore, it could be concluded that for plant phytochemical extraction, an alcoholic aqueous solvent is generally the most suitable. Nonetheless, the specific characteristics of the plant and phytochemicals should be considered before applying a particular type of solvent. As a case in point, Maurya et al. [145] produced *Bixa orellana* seed extract using ethanol mainly due to the primary phytochemical *cis*-bixin being water insoluble.

Temperature in Plant Extraction

The temperature applied is also a crucial factor in the plant extraction process as it can greatly impact the yield and quality of phytochemicals and, thus, affect the nanoparticle synthesised. As listed in Table 1, the temperature for extraction may range from room temperature to 100 °C. As an example of room-temperature extraction, Pilaquinga et al. [100] subjected pre-washed, oven-dried, and ground *Solanum mammosum* fruits to maceration with DI-H₂O at room temperature with constant agitation for an hour, while, as an example of the highest temperature, Hu et al. [141] extracted *Rhodiola rosea* rhizome powder by heating with DI-H₂O at 100 °C for 30 min. The temperature applied has a directly proportional relationship with solubility and diffusion. Nevertheless, when the temperature surpasses a particular threshold, it might lead to several problems such as solvent loss, introduction of impurities in the produced extract, and decomposition of thermolabile phytochemicals. For instance, when synthesizing Ag and Au nanoparticles from *Impinella anisum* seeds extracted at temperatures ranging from 25 to 60 °C, high surface plasmon resonance (SPR) peak intensities accompanied the raising of temperature due to the increased diffusion rate of the solvent, which destroyed the plant cell structure. However, when temperatures in the range of 60 to 85 °C were used, reduction in SPR was observed due to the decomposition of some thermolabile phytochemicals [167].

Extraction Time in Plant Extraction

Extraction time is another synergic factor that can greatly affect the phytochemicals extracted. Durations reported in the literature range from 200 s to a week; in addition, it can also be observed that the higher the temperature applied, the lower the extraction duration, and vice versa (Table 1). At the short end, Yallappa et al. [74] conducted an extraction of *Jasminum sambac* leaves in DS-H₂O assisted by microwave irradiation for 200 s. Meanwhile, for the longest duration, Yulizar et al. [159] macerated *Theobroma cacao* seed bark powder in methanol with stirring for a week. Extending the extraction duration can improve extraction efficiency as the mass transfer coefficient between plant components and solvent increases; accordingly, longer extractions can boost the quantities of extracted

phytochemicals and so enhance the formation of subsequently synthesised nanoparticles. However, such phenomena are restricted to within a certain time range, as when equilibrium has been reached inside and outside of the plant components, the extraction efficiency will not be further improved and could even worsen if the extraction period is excessively prolonged [4,167]. For example, extraction of *Impinella anisum* seeds for 60 min results in the greatest band intensity for subsequently produced nanoparticles, and band intensity then declines as the extraction duration increases due to the oxidation and thermal decomposition of phytochemicals [167]. Therefore, attentive consideration should be made regarding the duration of, and temperature during, phytochemical extraction.

Filtration and Preservation

After extraction, the next step is filtration, in which solid components are removed from the plant extract. There are many filtration techniques in use, as illustrated in Figure 1.

Following filtration, the obtained extracts are preserved for nanomaterial-synthesis research. Preservation is mainly achieved via refrigeration, directly using the extract for nanoparticle synthesis, or storing the extract in a container/environment with or without special conditions such as airtightness and light exclusion so as to avoid any manner of the oxidation or photodegradation of the phytochemicals. The temperature of refrigeration is mainly 4 °C as it was found that this temperature can best preserve the quality of *Ananas comosus* juice; moreover, increasing storage duration and temperature can greatly reduce the phytochemicals within the obtained plant extract [168]. Therefore, in the green synthesis of Cu-NMs, the freshness of the plant extract is very significant. Once a plant extract is produced, it should be utilised for nanoparticle synthesis as soon as possible and, in the interim, stored at low temperature.

Finally, the obtained plant extract is prepared for the synthesis of nanomaterials; for example, Nasrollahzadeh et al. [85,169] produced *Thymus vulgaris* leaf extract and used it to synthesise CuO and Cu nanoparticles, as shown in Figure 2.

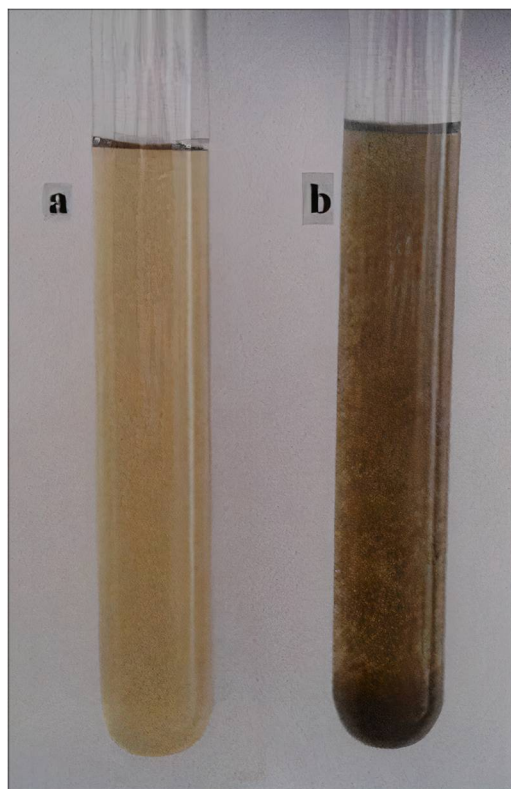


Figure 2. (a) *Thymus vulgaris* leaf extract and (b) solution after green synthesis of CuO nanoparticles. Adapted with permission from Ref. [85]. 2016, Elsevier.

It is worth knowing that, although the production of other type of nanomaterials via green synthesis methods are referenced in this review, the plant extraction methods mentioned above are compatible in Cu-NMs synthesis.

Although the above paragraphs generalised the parameters and methods for plant extraction, there is no one best universal extraction method and parameter set for extracting all phytochemicals from all plant components. The final selections should depend on the type of plant, the plant component, and any industrial requirements.

Next, this review covers the synthesis of Cu-NMs using plant extracts. There are several factors that need to be taken into account to ensure the successful production of nanomaterials, including reaction time, temperature, pH, and the extract/precursor used; these will all influence the size and geometry of the nanomaterial produced. Table 3 summarises previously reported works on the synthesis of Cu nanomaterials using plant extracts.

Table 3. Summary of plant-mediated Cu nanomaterial synthesis: plant extract type, key compounds, Cu precursors, synthesis time and temperature, reaction completion colour, and the Cu nanomaterial product, geometry, and size.

Plant	Cu Precursor	Synthesis Time	Synthesis Temperature (°C)	Key Compounds	Colour of the Product	Nanomaterials	Size (nm)	Geometry	Reference
Leaves									
<i>Agrimoniae herba</i>	<ul style="list-style-type: none"> • K₂PtCl₆ • CuSO₄ 	<ul style="list-style-type: none"> • 4 h • 8 h • 16 h • 24 h 	65	<ul style="list-style-type: none"> • Flavonoids 	-	<ul style="list-style-type: none"> Core-shell Cu-core Pt-shell 	30	Spherical	[170]
<i>Azadirachta indica</i>	<ul style="list-style-type: none"> • Cu(NO₃)₂ • AgNO₃ • ammonium molybdenate 	<ul style="list-style-type: none"> Stage 1—26 h Stage 2—1 h 	<ul style="list-style-type: none"> Stage 1—none Stage 2—500 (calcination) 	-	-	<ul style="list-style-type: none"> CuO nanoparticles Ag-CuO nanoparticles Mo-CuO nanoparticles Ag-Mo-CuO nanoparticles 	<ul style="list-style-type: none"> - - - 12 	Nanoflake	[171]
<i>Carica papaya</i>	<ul style="list-style-type: none"> • CuSO₄·5H₂O 	24 h	50–60	<ul style="list-style-type: none"> • Flavonoids • Phenolics 	Green to blackish brown	CuO nanoparticles	<50	Spherical	[68]
<i>Carica papaya</i>	<ul style="list-style-type: none"> • AgNO₃ • Cu(NO₃)₂ 	2 h	90	-	Light yellow green to olive green precipitate	Bimetallic Ag-Cu alloy	TEM-90-150 DLS-420.7	Tentacle-like	[172]
<i>Cyclea peltata</i>	<ul style="list-style-type: none"> • FeSO₄·7H₂O • CuSO₄·5H₂O 	4 h	Room temperature	<ul style="list-style-type: none"> • Carbohydrates • Amino acids • Alkaloids • Flavonoids • Saponins • Gallotannins 	Light yellow to green	<ul style="list-style-type: none"> Core-shell Cu-core Fe-shell 	45–50	Spherical	[173]
<i>Eclipta prostrata</i>	<ul style="list-style-type: none"> • Cu (CH₃COO)₂ 	24 h	Room temperature	-	-	Cu nanoparticles	28–45	Spherical, hexagonal, cubical	[71]
<i>Magnolia kobus</i>	<ul style="list-style-type: none"> • CuSO₄·5H₂O 	-	<ul style="list-style-type: none"> 95 25 60 	<ul style="list-style-type: none"> • Terpenoids • Reducing sugars 	-	Cu nanoparticles	<ul style="list-style-type: none"> 37–91 110 90 	Spherical	[75]
<i>Ocimum tenuiflorum</i>	<ul style="list-style-type: none"> • Cu (NO₃)₂ • Ag (NO₃)₂ 	6 h	80	-	Brownish blue	<ul style="list-style-type: none"> Core-shell CuO-shell Ag-core 	<ul style="list-style-type: none"> Ag core: 28–30 CuO shells: 6–10 	Spherical	[174]

Table 3. Cont.

Plant	Cu Precursor	Synthesis Time	Synthesis Temperature (°C)	Key Compounds	Colour of the Product	Nanomaterials	Size (nm)	Geometry	Reference
Leaves									
<i>Opuntia ficus-indica</i>	<ul style="list-style-type: none"> • AgNO₃ • Cu(NO₃)₂ 	1 h	55	<ul style="list-style-type: none"> • Ascorbic acid 	Slight green shade Slight blue shade	Core-shell Ag-coreCu-shell Bimetallic Ag-Cu alloy	10–20	Ellipsoidal -	[175]
<i>Origanum vulgare</i>	<ul style="list-style-type: none"> • Cu(NO₃)₂·3H₂O • Ni(NO₃)₂·6H₂O • Co(NO₃)₂·6H₂O 	Until alteration of colour	40	<ul style="list-style-type: none"> • Phenolic compounds • Water-soluble glycosides • Rosmarinic acid • Water-soluble glycosides • Caffeic acid • Protocatechuic acid • Glycoside protocatechuic acid • Derivatives of rosmarinic acid • 2-caffeoyloxy-3-[2-(4-hydroxybenzyl)-4,5-dihydroxy]phenylpropionic acid • Flavonoids 	Dark greenish-brown	Trimetallic Cu-Co-Nialloy	28.25	Nanoflake	[176]
<i>Pisonia grandis</i>	<ul style="list-style-type: none"> • Zn(NO₃)₂·6H₂O • Mg(NO₃)₂·6H₂O • Cu(NO₃)₂·9H₂O 	Stage 1—4 h	Stage 1—80 Stage 2—450 (calcination)	<ul style="list-style-type: none"> • Flavonoids 	Green to brownish black	Zn-Mg-Cu oxide nanocomposites	50	Cubic	[177]
<i>Plantago asiatica</i>	<ul style="list-style-type: none"> • CuCl₂·2H₂O 	5 min	80	<ul style="list-style-type: none"> • Polyphenolics 	Dark	Cu nanoparticles	7–35	Spherical	[79]
<i>Tabernaemontana divaricate</i>	<ul style="list-style-type: none"> • CuSO₄ 	7–8 h	100	<ul style="list-style-type: none"> • Enzymes • Proteins 	Brownish black	CuO nanoparticles	46 ± 4	Spherical	[84]
<i>Thymus vulgaris</i>	<ul style="list-style-type: none"> • CuCl₂·2H₂O 	5 min	60	<ul style="list-style-type: none"> • Polyphenolics 	Change from yellow to dark brown	CuO nanoparticles	<30	-	[85]
<i>Vitex negundo</i>	<ul style="list-style-type: none"> • AgNO₃ • CuSO₄ 	24 h	-	-	Green to Brown	Bimetallic Ag-Cu nanoparticles	60	Spherical	[178]

Table 3. Cont.

Plant	Cu Precursor	Synthesis Time	Synthesis Temperature (°C)	Key Compounds	Colour of the Product	Nanomaterials	Size (nm)	Geometry	Reference
Leaves									
Fruits									
<i>Crataegus pentagyna</i>	<ul style="list-style-type: none"> • FeCl₃·6H₂O • FeCl₂·4H₂O • Ag(NO₃) • Cu(NO₃)₂·3H₂O • tetra ethyl orthosilicate 	-	Room temperature	-	-	Fe ₃ O-SiO ₂ -Cu ₂ O-Ag nanocomposites	55–75	Spherical	[93]
<i>Piper retrofractum</i>	<ul style="list-style-type: none"> • CuSO₄·5H₂O 	60 min	60	<ul style="list-style-type: none"> • Flavonoids • Phenolic compounds • Piperidine alkaloids • Phenylpropanoids • Amides 	Dark green	Cu nanoparticles	2–10	Spherical	[179]
<i>Prunus nepalensis</i>	<ul style="list-style-type: none"> • CuSO₄ 	Overnight	Room temperature	-	Light green to brown and then to pink	Cu nanoparticles	35–50	Centred cubic	[180]
<i>Rosa canina</i>	<ul style="list-style-type: none"> • Cu (CH₃COO)₂ 	1 h	100	-	Dark brown	CuO nanoparticles	15–25	Spherical	[181]
<i>Rubus glaucus</i>	<ul style="list-style-type: none"> • Cu(NO₃)₂·3H₂O 	6 h	75–80	<ul style="list-style-type: none"> • Flavonoids • Phenolic compounds 	-	CuO nanoparticles	45	Spherical	[182]
<i>Syzygium alternifolium</i>	<ul style="list-style-type: none"> • CuSO₄·5H₂O 	2 h	50	-	-	CuO nanoparticles	2–21	Spherical	[101]
<i>Ziziphus spina-christi</i>	<ul style="list-style-type: none"> • CuSO₄ 	-	80	<ul style="list-style-type: none"> • Polyphenolic compounds 	Green to reddish brown	Cu nanoparticles	5–20	Elongated spherical	[183]
Peelings									
<i>Carica papaya</i>	<ul style="list-style-type: none"> • Cu(NO₃)₂·3H₂O 	Stage 1—none Stage 2—2 h	Stage 1—70–80 Stage 2—450 (calcination)	<ul style="list-style-type: none"> • Phenolic compounds • Flavonoids • Catechins 	Greenish-blue to green to dark green to black powder	CuO nanoparticles	85–140	Agglomerated spherical	[26]
Cavendish banana	<ul style="list-style-type: none"> • Cu(NO₃)₂·3H₂O 	Stage 1—none Stage 2—2 h	Stage 1—Boiling Stage 2—400	-	Brown paste to black powder	CuO nanoparticles	50–85	Agglomerated spherical	[184]

Table 3. Cont.

Plant	Cu Precursor	Synthesis Time	Synthesis Temperature (°C)	Key Compounds	Colour of the Product	Nanomaterials	Size (nm)	Geometry	Reference
Leaves									
<i>Citrus paradisi</i> (grapefruit)	• Anhydrous CuSO ₄	Stage 1—20 min Stage 2—72 h	Stage 1—70 Stage 2—room temperature	-	Brown precipitate	Cu nanoparticles	56–59	Spherical	[185]
<i>Citrus reticulata</i>	• CuSO ₄ ·5H ₂ O	10 min	25 ± 2 30 40 50	-	Brown	Cu nanoparticles	54–72	Spherical	[186]
<i>Punica granatum</i>	• CuSO ₄	Stage 1—10 min Stage 2—4 h	Stage 1—80 Stage 2—40	-	-	Cu nanoparticles	15–20	Spherical	[187]
Flowers									
<i>Acacia caesia</i>	• AgNO ₃ • CuNO ₃ • ZnO nanoparticles	-	Stage 1—none Stage 2—400 (calcination)	-	-	Ag-Cu-ZnO nanocomposite	Ag -7 Cu-12 ZnO-none	Spherical	[188]
	• CuNO ₃ • ZnO nanoparticles					Cu-ZnO nanocomposite	14		
<i>Aglaia elaeagnoides</i>	• Cu(NO ₃) ₂ ·3H ₂ O	5 min	Room temperature	• Phenolic compounds • Proteins	Light brownish red to brick red	CuO nanoparticles	3–54	Spherical	[118]
<i>Aloe vera</i>	• Cu (CH ₃ COO) ₂	Stage 1—30 min Stage 2— overnight	Stage 1—50 Stage 2—room temperature	-	Light green to dark green	Cu nanoparticles	40	Spherical	[120]
<i>Azadirachta indica</i>	• CuSO ₄ ·5H ₂ O	1 h	80	• Terpenoids • Terpenes • Flavonoids • Alkaloids • Carotenoids	Light blue to light green to dark yellow to brown precipitate	Cu nanoparticles	5	Spherical	[122]
<i>Bougainvillea sp.</i>	• Cu (CH ₃ COO) ₂	-	-	-	Blue to black-blue colour	CuO nanoparticles	12–20	Spherical	[188]
<i>Calendula sp.</i>	• Fe ₃ O ₄ nanoparticles • Cu (NO ₃) ₂ ·3H ₂ O	Stage 1—1 h Stage 2—6 h	Room temperature	-	-	Cu-Fe ₃ O ₄ nanocomposite	20–40	Globular	[123]

Table 3. Cont.

Plant	Cu Precursor	Synthesis Time	Synthesis Temperature (°C)	Key Compounds	Colour of the Product	Nanomaterials	Size (nm)	Geometry	Reference
Leaves									
<i>Eichhornia crassipes</i>	• CuSO ₄	48 h	Room temperature	• Aromatic compounds like lawsone and phenol	Colourless to light red	Cu nanoparticles	12–15	Spherical	[189]
<i>Lantana camara</i>	• Cu (CH ₃ COO) ₂	Stage 1—10 min Stage 2—2 h	65	-	-	CuO nanoparticles	13–28	Spherical	[190]
Roots and Rhizomes									
<i>Asparagus adscendens</i>	• CuSO ₄ •5H ₂ O	1 h	Room temperature	-	Pale yellow to sky blue	Cu nanoparticles	10–15	Spherical	[191]
<i>Asparagus racemosus</i>	• Cu(NO ₃) ₂ •3H ₂ O	8 h	60	• Phenolic compounds	-	CuO nanoparticles	Diameter: 50–100 Length: 400–500	Rod-like	[192]
<i>Corallocarbus epigaeus</i>	• CuSO ₄	12 h	80–100	-	Deep blue to colourless and then to brick red and dark red	Cu nanoparticles	65–80	Spherical	[193]
<i>Polyalthia longifolia</i>	• CuSO ₄	30 min with stirring and 24 h storage	-	• Phenolic compounds • Flavonoids	Dark green colour	Cu, CuO ₂ , Cu ₂ O, and CuO nanoparticles	30	Spherical	[194]
<i>Rheum emodi</i>	• AgNO ₃ • Cu (CH ₃ COO) ₂	3 h	90	• Physcion • Chrysophanol • Aloe-emodin • Emodin • Chrysophanol glycoside	Light brown to black	Bimetallic Ag-Cu nanoparticles	40–50	Pseudo-spherical	[195]
	• Cu (CH ₃ COO) ₂	4 h	90		Blue to brown	Cu nanoparticles	-	-	
<i>Senna didymobotrya</i>	• CuSO ₄ •5H ₂ O	-	40 60 80	• Alizarin • Quercetin	-	Cu nanoparticles	5.55–63.60	Spherical	[196]
<i>Zingiber officinalis</i> <i>Curcuma longa</i>	• Copper sulphate	-	Room temperature	-	Straw yellow to sea green	Cu nanoparticles	Around 20–100	Spherical	[197]
Seeds									
<i>Caesalpinia bonducella</i>	• Cu(NO ₃) ₂ •3H ₂ O	Stage 1—5 h Stage 2—2 h	-	-	Stage 1—blue-coloured solution turned green Stage 2—dark brown precipitate	CuO nanoparticles	-	Rice-grain-shaped	[146]

Table 3. Cont.

Plant	Cu Precursor	Synthesis Time	Synthesis Temperature (°C)	Key Compounds	Colour of the Product	Nanomaterials	Size (nm)	Geometry	Reference
Leaves									
<i>Carum carvi</i>	-	-	-	-	-	Cu nanoparticles Fe ₃ O ₄ -Cu nanocomposite	37 62	Spherical Spherical	[198]
<i>Koeleruteria apiculata</i>	• CuCl ₂ ·2H ₂ O	24 h	-	-	Precipitate formation	Cu nanoparticles	20	Spherical	[199]
<i>Persea americana</i>	• CuSO ₄	6–7 h	45–50	• Flavonoids • Phenolic compounds	Brownish black	Cu nanoparticles	42–90	Spherical	[200]
<i>Punica granatum</i>	• CuCl ₂ ·2H ₂ O	Stage 1—10 min Stage 2—1–2 h Stage 3—4–6 h	Stage 1—60–70 Stage 2—60 Stage 3—room temperature	• Alkaloids • Flavonoids • Polyphenols	Stage 2—dull bluish brown colour Changed to dark green	Cu nanoparticles	40–80	Spherical	[154]
<i>Silybum marianum</i>	• FeCl ₃ ·6H ₂ O • CuCl ₂ ·2H ₂ O	5 h	60	• Flavonoids • Phenolic compounds	Dark solution and forming of precipitate	Cu-Fe ₃ O ₄ nanoparticles	8.5–60	Spherical	[201]
<i>Theobroma cacao</i>	• PdCl ₂ • CuCl ₂ ·2H ₂ O	2 h	50	• Flavonol antioxidants such as epicatechin, catechin	-	Pd-CuO nanoparticles	40	-	[202]
<i>Triticum aestivum</i>	• CuSO ₄ ·5H ₂ O	Stage 1—1 h Stage 2—10 min Stage 3—20 min	Stage 1—room temperature (25) Stage 2—sonication Stage 3—70	• Starch	Dark blue to dark brown	CuO nanoparticles	21–42	Spherical	[203]

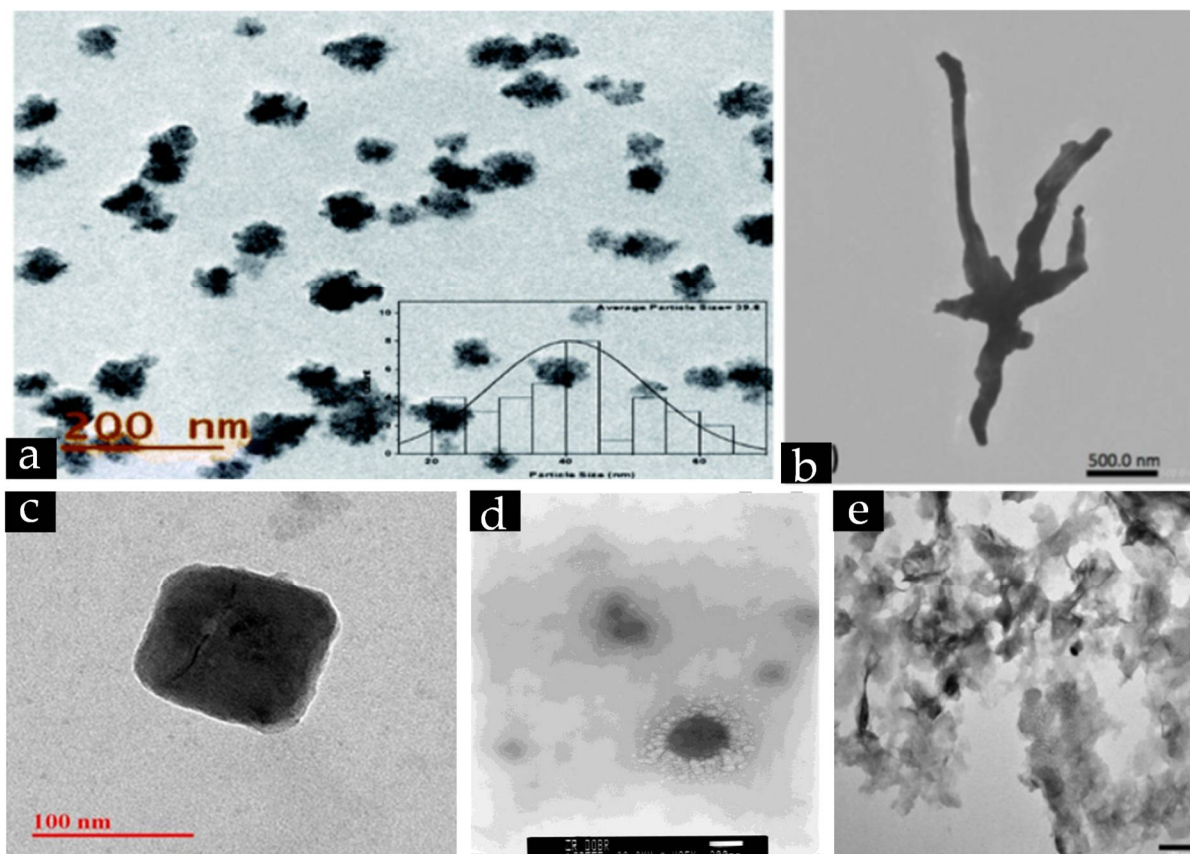


Figure 3. Representative TEM images of (a) spherical CuO nanoparticles synthesised using *Annona squamosa* seed extract. Reproduced from [204]. 2021 with permission from the Royal Society of Chemistry, (b) tentacle-like bimetallic Ag-Cu nanoparticles synthesised using *Carica papaya* extract. Adapted with permission from Ref. [172]. 2017, Elsevier, (c) cubical Cu nanoparticles synthesised from *Azadirachta indica* leaf extract. Adapted with permission from Ref. [65]. 2018, Elsevier; (d) SEM image of spherical Cu-Pt core shell nanoparticles synthesised using *Agrimoniae herba* extract. Adapted with permission from Ref. [170]. 2018, Elsevier; and (e) TEM image of Cu-Co-Ni trimetallic nanoalloy nanoflakes synthesised using *Origanum vulgare* leaf extract. Adapted with permission from Ref. [176]. 2020, MDPI.

3.2. Cu-NMs Synthesis Method

3.2.1. Production of High Tunable Cu-NMs

All extracts from plant components are composed of various types of phytochemicals such as flavonoids, phenolics, alizarin, quercetin, terpenoids, terpenes, alkaloids, carotenoids, and others. These phytochemicals can potentially be used for the synthesis of various types of Cu-based nanomaterials such as pure Cu nanoparticles, CuO nanoparticles, Cu-based nanocomposites, core-shell nanoparticles, and nanoalloys. For example, Ituen et al. [186] used *Citrus reticulata* peel extract to produce spherical Cu nanoparticles with sizes of 54 and 72 nm. Similarly, *Azadirachta indica* flower extract has been used to produce pure spherical 5 nm Cu nanoparticles [122], and *Thymus vulgaris* leaf extract to produce CuO nanoparticles with spherical morphology and a particle size less than 30 nm [85]. In addition, Dobrucka and Dlugaszewska synthesised 30 nm spherical bimetallic Pt-Cu core-shell particles with Cu as the core and Pt as the shell from the ethanolic extract of *Agrimoniae herba* leaves [170]. As an example of root-extract-mediated nanoparticle synthesis, Pallela et al. [192] successfully produced rod-shaped CuO nanoparticles with diameters of 50–100 nm and lengths of 400–500 nm from *Asparagus racemosus* root extract. Regarding nanoparticle synthesis from fruits, Ebrahimzadeh et al. [93] produced

spherical $\text{Fe}_3\text{O}_4/\text{SiO}_2/\text{Cu}_2\text{O}-\text{Ag}$ nanocomposites with diameters of 55 and 75 nm from *Crataegus pentagyna* fruit extract. Meanwhile, Sajadi et al. [201] used *Silybum marianum* seed extract to produce agglomerated $\text{Cu}/\text{Fe}_3\text{O}_4$ nanoparticles with sizes of 8.5–60 nm and magnetic properties.

As indicated in Table 3, the sizes of nanoparticles produced using plant-mediated synthesis ranges from 2 to 150 nm. On the other hand, the morphology of the produced nanoparticles is predominantly spherical [172,205,206] with some having other shapes such as hexagonal, cubical [65,71], ellipsoidal [175], tentacle-like [172], or nanoflake [171,176] (Table 3 and Figure 3). Several characterization methods are used in determining the size and morphology of nanoparticles, with the preeminent being scanning electron microscopy (SEM), transmission electron microscopy (TEM), and dynamic light scattering (DLS). It should be noted that the findings elucidated by each characterization method might have some discrepancies. For instance, Rosbero and Camacho observed synthesised Ag/Cu nanoparticles to have a size of 420.70 nm according to DLS, but a size range of 90–150 nm by TEM [172]. This discrepancy is attributable to the presence of solvent molecules on the nanoparticle surface and DLS only determining the hydrodynamic size of the particles rather than the core diameter. That is to say, when there is a hydration layer surrounding the nanoparticles, only the solvated particle size is indicated by a particle's diffusional characteristics [172,186]. Hence, to obtain the most accurate results and perform effective quality control of nanomaterials, multiple characterization methods should be employed.

Overall, it can be observed that Cu -NMs produced via plant-mediated synthesis feature size and morphology tunability comparable to those obtained with chemical synthesis methods. Specifically, tunability can be achieved via altering parameters such as the precursor concentration, plant extract, reaction time, and the temperature applied during nanoparticle synthesis.

3.2.2. Precursor

As listed in Table 3, most studies to date have utilised CuSO_4 [188,202,205], $\text{Cu}(\text{NO}_3)_2$ [120,186,194], and CuCl_2 [79,199] as the Cu precursor, while some used copper acetate ($\text{Cu}(\text{OAc})_2$) [71,181]. Interestingly, for some multi-metallic nanoparticles (nanoalloys, core-shell particles, and nanocomposites), multiple precursors have been utilised and the type of nanoparticle formed depends on the methodology. For example, Cu-Co-Ni trimetallic nanoalloy was synthesised using *Origanum vulgare* leaf extract and the precursors of $\text{Cu}(\text{NO}_3)_2 \cdot 3\text{H}_2\text{O}$, $\text{Ni}(\text{NO}_3)_2 \cdot 6\text{H}_2\text{O}$, and $\text{Co}(\text{NO}_3)_2 \cdot 6\text{H}_2\text{O}$ [176], while bimetallic Pt-Cu core-shell structures with Cu as core and Pt as shell were synthesised from *Agrimoniae herba* leaf ethanolic extract with K_2PtCl_6 and CuSO_4 as the precursors [170]. Basically, multiple metallic precursors are mixed with a plant extract and stirring and heat applied to yield multi-metallic nanoparticles. Generally, a combination of two metals will lead to the synthesis of alloy or core-shell nanoparticles. Which form of Cu-NM is produced can be determined based on SPR from UV–visible analysis: if a single SPR is found, an alloy was formed, while if two independent and continuous peaks are evident, a core-shell-type structure resulted [172]. For instance, Ag/Cu nanoparticles produced via bio-reduction with *Carica papaya* extract exhibited a single peak at 776 nm as the maximum absorption, suggesting an alloyed structure [172]. Cu -based nanocomposites are also able to be synthesised via plant-mediated methods; Ebrahimzadeh et al. [93] produced spherical $\text{Fe}_3\text{O}_4/\text{SiO}_2/\text{Cu}_2\text{O}-\text{Ag}$ nanocomposites of 55 and 75 nm in size using *Crataegus pentagyna* fruit extract with $\text{FeCl}_3 \cdot 6\text{H}_2\text{O}$, $\text{FeCl}_2 \cdot 4\text{H}_2\text{O}$, $\text{Ag}(\text{NO}_3)$, $\text{Cu}(\text{NO}_3)_2 \cdot 3\text{H}_2\text{O}$, and tetra ethyl orthosilicate.

In addition to precursor choice, the concentration of precursor applied in the reaction also plays an important role in determining the Cu-NMs synthesised. Lee et al. [75] used *Magnolia kobus* leaf extract to produce spherical Cu nanoparticles, mixing it with $\text{CuSO}_4 \cdot 5\text{H}_2\text{O}$ at 0.5, 1, and 2 mmol/L and reducing the Cu ions to atoms. Given constant temperature and plant extract concentration, the time required to achieve a conversion rate of more than 90% was 1600, 1400, and 200 min for the concentrations of 0.5, 1, and 2 mmol/L, respectively. Therefore, it could be concluded that a higher precursor concentration can accelerate nanoparticle formation. In addition, a study that performed precursor

optimization for the green synthesis of Cu nanoparticles from *Senna didymobotrya* root extract utilised $\text{CuSO}_4 \cdot 5\text{H}_2\text{O}$ at concentrations of 0.0125, 0.03125, and 0.05 M [196]. This study revealed that the higher the precursor concentration, the higher the nanoparticle size. The authors noted this could be due to a low concentration of Cu ions reducing the chance of Cu-Cu interactions and, hence, reducing agglomeration [196]. Thus, the formation rate and size of synthesised nanoparticles can be controlled via altering the precursor concentration. However, the balance between conversion rate (nanoparticle formation) and nanoparticle size should be taken into account when carrying out green-synthesis research to ensure the desired nanoparticle is produced while also achieving a highly productive and efficient synthesis process.

3.2.3. Plant Extract

The plant extract utilised is also another major factor that should be considered in plant-mediated Cu-NM synthesis. A variety of plant extracts have demonstrated great impact on the synthesis of Cu-NMs (Table 3). In a study examining the effect of extract concentration on nanoparticle synthesis rate and characteristics, *Magnolia kobus* leaf extract at a range of concentrations (5–20%) was used to produce spherical Cu nanoparticles [75]. The highest synthesis rate was obtained with an extract concentration of 20%, while high average particle sizes were obtained for both the lowest (5%) and highest (20%) extract concentrations, with diameters of 91 and 82 nm, respectively. Meanwhile, an extract concentration of 15% produced nanoparticles with diameter 37 nm, which was the smallest among all the results [75]. The reason for the production of large nanoparticles from high extract concentrations is due to the excessive abundance of capping materials promoting the aggregation of Cu particles owing to the interaction between nanoparticles that are surrounded with proteins and metabolites (reducing sugar, terpenoid, and other metabolites) [75]. Therefore, it can be concluded that if a high yield of a small Cu nanoparticle is required, the leaf extract concentration should be optimised before conducting the plant-mediated synthesis process at scale, whereas if the most rapid production is required, a high concentration of plant extract should be applied.

3.2.4. Temperature

Aside from material inputs, the temperature applied during plant-mediated Cu-NM synthesis is also an essential parameter to be investigated. According to Table 3, the temperatures utilised in existing reports range between 25 and 100 °C. For example, temperatures of 25 ± 2, 30, 40, and 50 °C have been used for Cu nanoparticle production from *Citrus reticulata* peel extract [186], and 100 °C for CuO nanoparticle synthesis from *Rosa canina* fruit extract [181]. Notably, the use of different temperatures can greatly impact the Cu-NM synthesis process. For example, in the abovementioned study using *Citrus reticulata* peel extract combined with $\text{CuSO}_4 \cdot 5\text{H}_2\text{O}$ [186], successful bio-reduction and nanoparticle production was indicated by a colour change to brown with absorption at 442 nm (Figure 4). At reaction temperatures of 25, 30, 40, and 50 °C with a constant pH, achieving this endpoint required 72 h, 60 h, 10 h, and 105 min, respectively. Therefore, plant-mediated synthesis of Cu-NMs is a temperature-dependent process with a positive proportional relationship: the higher the temperature, the higher the rate of conversion from Cu ion to Cu metal.

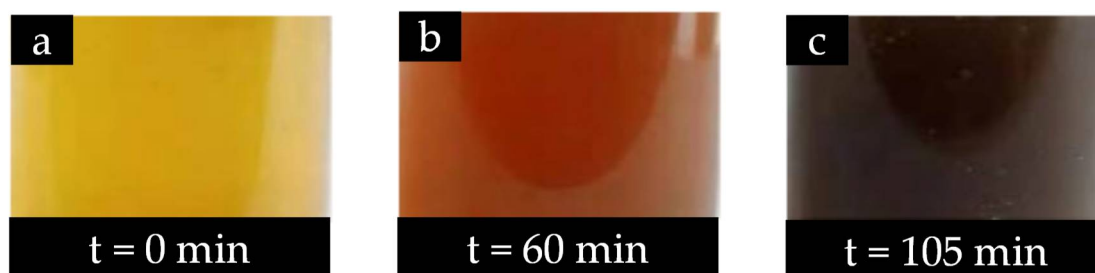


Figure 4. Colour change over time during the reaction between *Citrus reticulata* peel extract and $\text{CuSO}_4 \cdot 5\text{H}_2\text{O}$ at (a) 0 min, (b) 60 min and (c) 105 min. Adapted with permission from Ref. [186]. 2020, Elsevier.

Interestingly, nanoparticle synthesis rate and size behave differently under a given reaction temperature increment, as the conversion rate increases whereas nanoparticle size decreases with increasing reaction temperatures. For instance, as mentioned above, Lee et al. [75] synthesised Cu nanoparticles using *Magnolia kobus* leaf extract and observed a size reduction from 110 nm at low temperature (25 °C, conversion rate 70%) to 37 nm at high temperature (95 °C, conversion rate ~80–100%). The rationale behind such phenomena is that the increasing temperature improves the reaction rate. When the reaction rate is increased, Cu ions in the reaction solution are only able to be consumed for the formation of nuclei; the secondary reduction process on the nuclei is avoided. Thus, larger nanoparticles cannot be produced at higher temperatures [75,196]. Consequently, it can be concluded that nanomaterials synthesis is temperature-dependent, but the size of nanomaterials has a negative proportional relationship with temperature such that producing nanoparticles with a larger size necessitates utilising a lower temperature.

There have been studies conducted on further calcination of metal oxides at temperatures ranging from 400 to 500 °C after the synthesis process (Table 3) [27,179,190]. One of the purposes of calcination is to produce stable metal oxides or metal oxide nanocomposites through oxidation [177]. For example, Suresh et al. [177] used *Pisonia grandis* leaf extract to synthesise Zn-Mg-Cu oxide nanocomposites, then calcinated them at 450 °C to obtain mixed metal oxide nanocomposites. In addition to producing stable oxides, increasing calcination temperature can boost the size of Cu-NMs and produce black precipitates of agglomerated cubical nanomaterials, where uncalcinated nanomaterials have elongated morphology [205].

3.2.5. pH

Solution pH is also a very significant factor in plant-mediated nanomaterial synthesis as it can affect the synthesis rate and products. Mechanistically, the importance of pH is due to the reducing and stabilizing agents being greatly dependent on the phytochemicals within the plant extract, which might be readily affected by pH. Generally, the best pH values for plant-mediated nanomaterial synthesis are in the range of pH 7–9, and varying the pH will alter the nanoparticle synthesised [14]. Nagar and Devra utilised *Azadirachta indica* leaves for Cu nanoparticle synthesis at various pH values [65]. They found that nanoparticle synthesis is more effective at higher pH and abolished in an extreme acidic environment, such as pH 4.7. A solution with pH 6 produced small-sized nanoparticles of 56 nm, while in an alkaline environment of pH 9.3, the nanoparticles produced were of size 73 nm. In an acidic environment, the phytochemicals in the plant extract might be inactivated [65]. In addition, lower pH can cause nanoparticles to experience high electrostatic repulsion which reduces the chances of agglomeration and, thus, yields nanomaterials of smaller size [196]. Conversely, in a more alkaline condition such as pH 10, the low electrostatic forces of the nanoparticles allow further particle growth and agglomeration, which produces larger nanomaterials [65,196]. It is worth noting that during the plant-mediated synthesis process, the pH of the medium will drop as the Cu^{2+} ions cause oxidation of the plant extract, leading to the release of H^+ ions and, hence, acidification; this is also another important aspect to be considered by researchers carrying out plant-mediated nanomaterial synthesis [65].

Therefore, it is necessary to achieve a balance in producing nanoparticles with a desired size while maintaining high nanomaterial productivity.

3.2.6. Reaction Time

In terms of duration, it can be seen that the range of reaction times in the literature is relatively large, ranging from as low as 5 min to as long as 72 h. The duration is not as impactful compared to the other parameters mentioned above [205]. Although a long synthesis duration allows improvement in the nanomaterial nucleation rate, the reaction rate will not continue to increase after the optimum time has been reached. In some cases, prolonging the incubation might even cause nanomaterial aggregation [206]. In fact, other parameters such as temperature, precursor, and type of plant extract can greatly impact the time needed to achieve complete conversion from metallic ions (Cu and other ions depending on the type of nanomaterial being produced) to metallic atoms and, finally, nanomaterials, as was mentioned previously in relation to other parameters. However, compared with other materials such as Au, Ag, and Pt, Cu forms nanoparticles relatively slowly as the initiation of Cu nucleus formation is much more difficult [75]. Hence, the green synthesis of Cu nanoparticles necessitates longer reaction times in order to achieve 100% conversion.

3.2.7. Indication of Cu-NMs Production

During the production of Cu-NMs, a successful reaction is indicated by the colour alteration of the reaction solution. For example, *Thymus vulgaris* leaf extract mixed with $\text{CuCl}_2 \cdot 2\text{H}_2\text{O}$ with constant stirring at 60 °C undergoes a change in colour from yellow to dark brown, as shown in Figure 2. In addition, calcination will also change the colour of nanomaterials produced. *Carica papaya* peel extract combined with $\text{Cu}(\text{NO}_3)_2 \cdot 3\text{H}_2\text{O}$ and heated at 70–80 °C changes colour from greenish-blue to green and finally produces a dark green paste. Upon calcination, a fine black-coloured powder was obtained and harvested as CuO nanoparticles [26].

4. Applications of Cu-NMs from Plant-Mediated Synthesis

After the synthesis reaction is completed, the obtained nanoparticles are washed, dried, and employed in applications. Cu-NMs synthesised using plant extracts have been utilised in two major areas, namely, biomedical and environmental remediation [31].

4.1. Biomedical

Plant-mediated Cu-NMs have demonstrated antimicrobial, antioxidant, and anticancer activities, and have potential as nano-sensors and in various medical applications. In this section, details and mechanisms pertaining to this area will be discussed.

4.1.1. Antimicrobial

Firstly, antibacterial activity has been observed for plant-mediated Cu-NMs [205] and can be attributed to several putative pathways. Bhavyasree and Xavier suggested that Cu-NMs, including both Cu and CuO nanoparticles produced via plant-mediated synthesis, can carry out antibacterial activity through a chemisorption-based mechanism [206]. This mechanism involves microbial adsorption to the nanoparticle surface, which has been bio-functionalised by phytochemicals during the plant-mediated synthesis process. The adsorption is mainly due to chemisorption via non-electrostatic forces (Van der Waals force and hydrogen bonding), which causes the destruction of the microbial cell wall and subsequent cell membrane damage, DNA breakage, and eventually cell death, as illustrated in Figure 5.

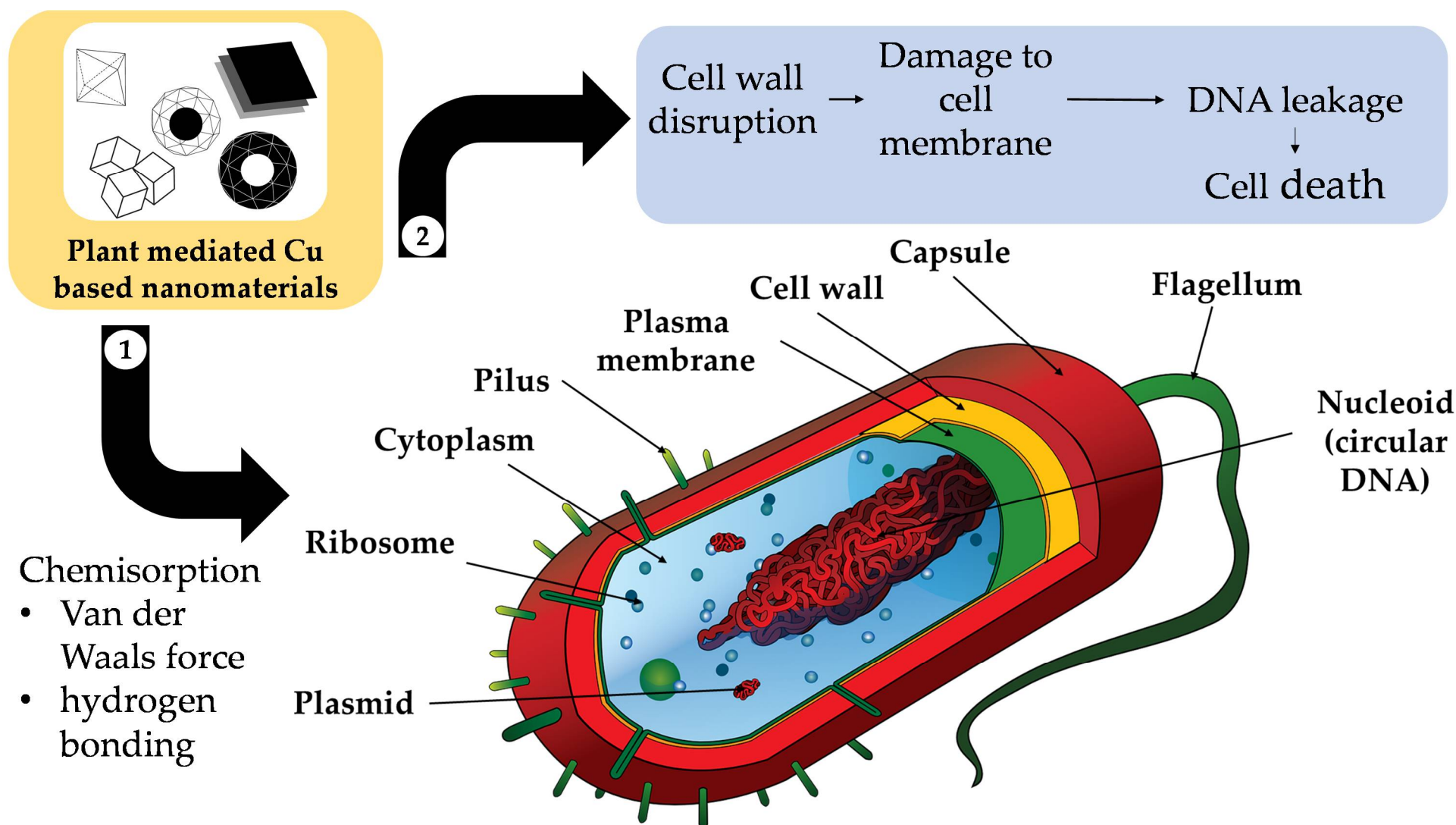


Figure 5. Diagram of the chemisorption-based mechanism of Cu-based nanomaterials' antimicrobial activity.

Another antibacterial mechanism is mediated by reactive oxygen species (ROS) and the release of Cu^{2+} ions [207]. First, the CuO nanoparticles are much smaller (being of a nanometre scale) than the micrometre-scale pores of bacterial cells, which allows them to easily penetrate the cells. In addition, Cu^{2+} ions are attracted toward bacterial cells due to the abundance of carboxyl and amine groups on the cell surface; this is another factor in antibacterial ability. However, the antibacterial interactions are different for Gram-positive and Gram-negative bacteria, as described in Figure 6a.

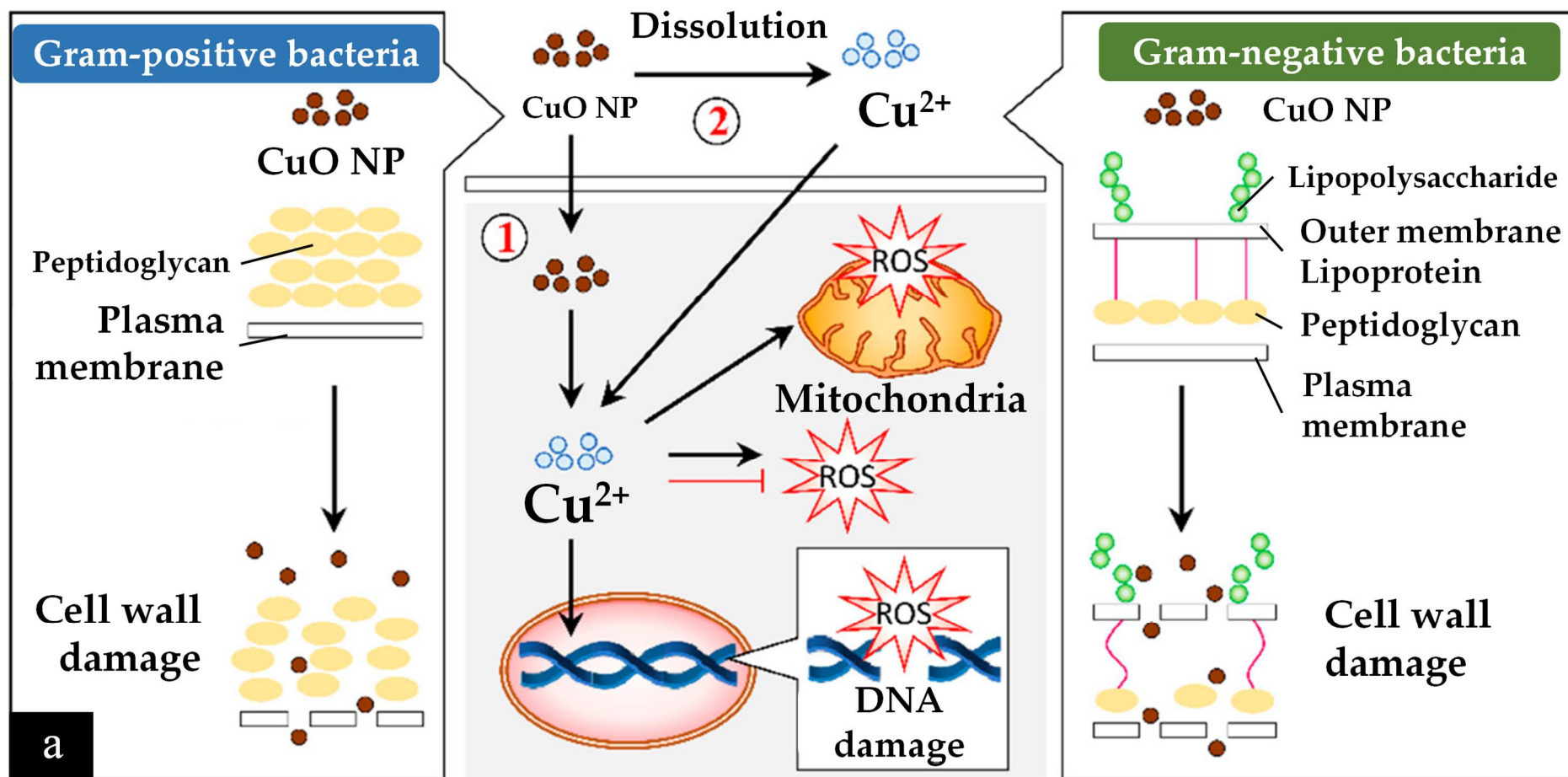


Figure 6. Cont.

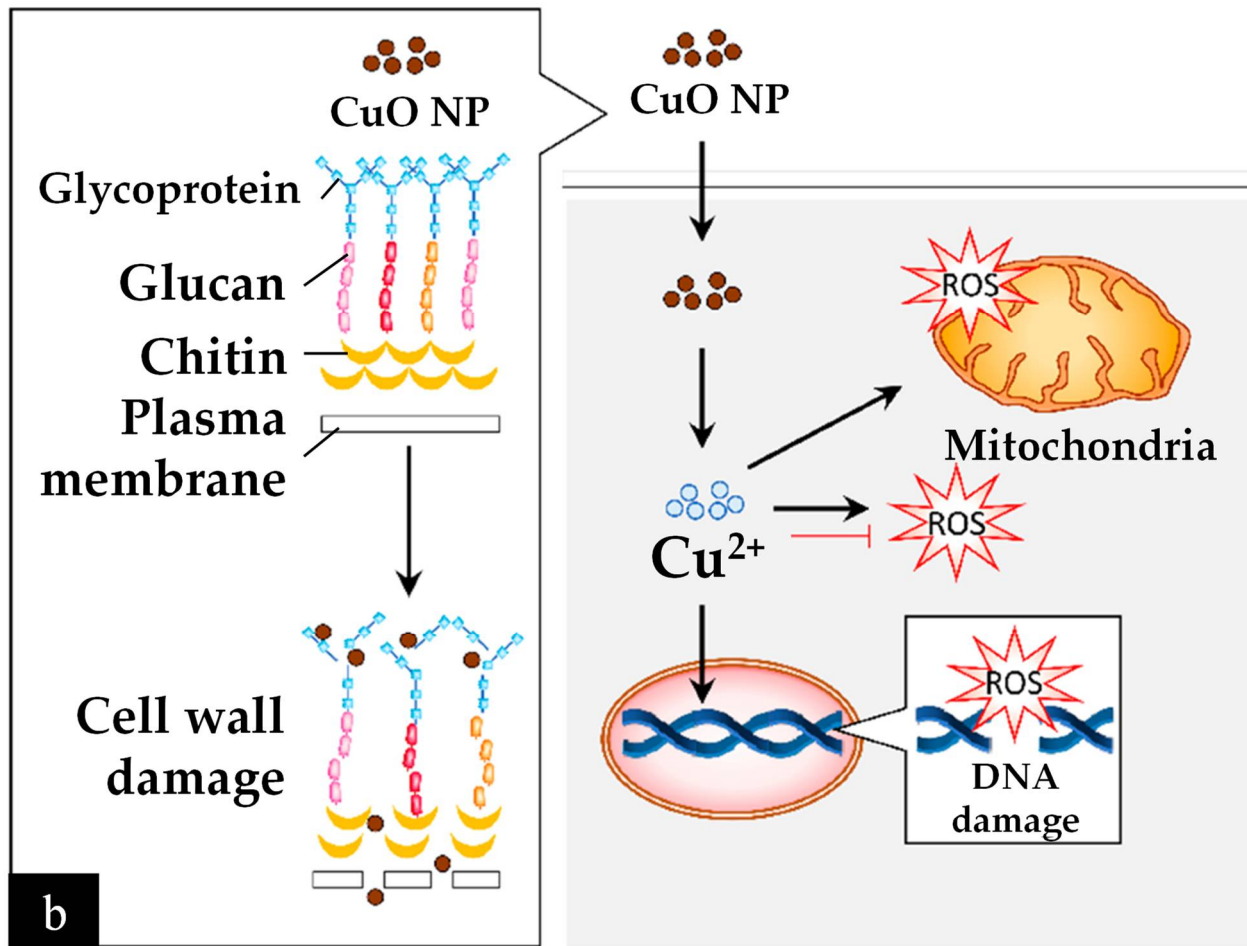


Figure 6. (a) Diagram of the respective mechanisms of CuO nanoparticle antibacterial activity in Gram-positive and Gram-negative bacteria and (b) diagram of the mechanism of CuO nanoparticle antifungal activity. Adapted with permission from Ref. [205]. 2020, MDPI.

After bypassing the cell wall, Cu^{2+} ions relocate intracellularly to the cytosol due to the internalization of CuO nanoparticles and Cu^{2+} ions, where they cause ROS to accumulate [205]. Consequently, DNA and mitochondria damage occur. Cu^{2+} ions within a bacterium may also stimulate cellular responses that lead to bactericidal activity. For example, radicals produced by CuO nanoparticles, such as superoxide and hydroxyl radicals, can have synergic effects in causing bacterial membrane destruction, DNA damage, attachment to ribosomes, oxidative injury, and protein and proton efflux pump damage; they can also prevent biofilm production [205,207].

Cu-NMs exert antibacterial activity through mechanisms similar to those of Cu and CuO nanoparticles. Generally, the antibacterial activity of nanomaterials is mainly owed to the induction of oxidative stress, such as through the production of free radicals and ROS. Notably, nano-sized particles will feature a smaller surface-to-volume ratio, harbour more surface defects due to oxygen vacancies, and feature greater electrostatic attraction and release of Cu^{2+} ions and generate more oxidative stress within the bacterial cells [178]. In addition, bimetallic nanoparticles can demonstrate a synergic effect with improved antibacterial ability. For example, bimetallic Ag and Cu nanoparticles produced by *Vitex negundo*-mediated synthesis demonstrate antibacterial activity when applied in a cellulose matrix via the disc method against both Gram-positive (*Escherichia coli*, *Pseudomonas*, *Klebsiella*) and Gram-negative (*Staphylococcus*, *Bacillus*) species [178]. Particles having an equal ratio of Ag and Cu (2.5 mM each) exhibited the greatest antibacterial ability, with a 9 mm zone of inhibition for all the tested species.

Secondly, Cu-NMs have also been demonstrated to possess antifungal activity. A number of fungi can cause infections in humans with severe symptoms, such as *Candida albicans* which can cause mucosal infections (oropharyngeal or vulvovaginal candidiasis), or *Trichophyton mentagrophytes* which can cause dermatophytosis [208,209]. Antifungal activity is more challenging to realise than antibacterial as a fungus cell has several layers of lipids within its cell wall which impede the penetration and internalization of Cu nanomaterials [205]. Although fewer publications exist regarding the antifungal testing of Cu nanomaterials synthesised by green methods, their hypothesised antifungal mechanism is based on altering the structure and function of fungal cell components [210]. That is, the nanoparticles first distort the cell wall and become internalised by the fungus (Figure 6b). After internalization, the same process of ROS generation and subsequent process disruption ensues as in bacteria, impacting DNA, mitochondria, replication, protein synthesis and other essential elements, eventually leading to cell death [205,210].

In one report of Cu-NM antifungal activity, Mali et al. [210] tested the efficacy of Cu nanoparticles derived from *Celastrus paniculatus* leaf extract against *Fusarium oxysporum*. Concentrations of 0.12%, 0.18% and 0.24% (*w/v*) Cu nanoparticles were found able to inhibit mycelial growth by $76.29 \pm 1.52\%$, $73.70 \pm 1.52\%$, and $59.25 \pm 0.57\%$, respectively, calculated via the following formula:

$$(\% \text{ inhibition rate}) = \frac{(Mc - Mt)}{Mc} \times 100 \quad (1)$$

where *Mc* represents mycelial growth in the control (with water) while *Mt* is mycelial growth under the Cu nanoparticle treatment. The inhibition rate was found to be dosage-dependent: the higher the Cu nanoparticle dosage, the higher the degree of inhibition.

Dobrucka and Dlugaszewska similarly studied the antibacterial and antifungal activities of Cu-Pt core-shell nanoparticles synthesised using *Agrimoniae herba* extract [170]. The nanoparticles were applied via the well-diffusion method to three species of bacteria, including *Staphylococcus aureus*, *Escherichia coli*, and *Pseudomonas aeruginosa*, and three of fungi: *Candida albicans*, *Trichophyton mentagrophytes*, and *Aspergillus fumigatus*; the authors then determined the minimal inhibitory concentration (MIC), minimal bactericidal concentration (MBC), and minimal fungicidal concentration (MFC) [170]. The Cu-Pt nanoparticles exhibited good inhibitory function on all tested bacteria and *Trichophyton Mentagrophytes*. The overall best antibacterial

and antifungal performances were obtained on *Staphylococcus aureus* (MIC of 16.7 and MBC of 33.3) and *Trichophyton mentagrophytes* (MIC and MFC of 26.7).

From the above reports, it can be concluded that plant-mediated Cu-NMs are suitable as antibacterial (for both Gram-positive and -negative) and antifungal agents. Such characteristics are useful in further broadening the application of Cu-NMs in the pharmaceutical and medical sectors.

In addition to direct antimicrobial effects, many plant-mediated Cu-NMs have also demonstrated antioxidant properties which also contribute to antibacterial and antifungal activities as a synergic factor [205]. Multiple mechanisms contribute to antioxidant ability, which are: (1) binding of transition metal ion catalysts, (2) reductive capacity, (3) radical scavenging activity, (4) decomposition of peroxides, (5) prevention of continued hydrogen abstraction, and (6) prevention of chain initiation.

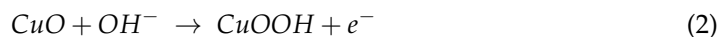
Interestingly, plant selection has been shown to impact the antioxidant ability of Cu-NMs. For example, Rehana et al. [211] synthesised nanoparticles using extracts of *Azadirachta indica*, *Hibiscus rosa-sinensis*, *Murraya koenigii*, *Moringa oleifera*, and *Tamarindus indica*, then tested their antioxidant capabilities with ABTS, DPPH, and hydrogen peroxide assays. *Tamarindus indica*-mediated nanoparticles were found to have the highest antioxidant activity, and *Moringa oleifera* the lowest, though still superior to CuO nanoparticles produced via a chemical method. Therefore, plant-mediated nanomaterials have much higher antioxidant ability as compared to chemical-mediated materials, and the plant used is an essential consideration for antioxidant purposes.

4.1.2. Nano-Sensor

Plant-extract-mediated Cu-NMs have also been utilised in the preparation of nano-sensors. Cu nanomaterials, such as CuO nanoparticles, are suitable for nano-sensor production owing to their characteristic high electron-transfer rate, superior catalytic activity, large surface area, high glucose selectivity in heterogenous samples (such as blood or urine), chlorine poisoning resistance, and corrosion resistance. For example, Ag-CuO core-shell nanoparticles produced using *Ocimum tenuiflorum* extract have been used for non-enzymatic glucose sensing with a screen-printed electrode [174]. The synthesised electrode provided good glucose-sensing performance with a sensitivity of $3763.44 \mu\text{AmM}^{-1}\text{cm}^{-2}$, linear range of 1 to 9.2 mM, detection limit of 0.006 mM ($S/N = 3$), and response time of less than 1 s. Moreover, the CuO-Ag core-shell-modified bio-nano-sensors demonstrated exceptional adhesion and structural strength along with great long-term stability for up to 60 days, exhibiting 99.2% of the initial value after one month with excellent repeatability and reproducibility.

The mechanism by which these nanoparticles sense glucose is based on electron transfer from the screen-printed electrode to the CuO nanoparticle core via the conduction band electrons of the Ag shell. This electron transfer occurs because the work function of CuO is bigger than that of Ag, and equalization of Fermi levels ensues after the materials come into electrical contact and the mobility of electrons is improved. The progression of current-induced charge carriers can boost electrocatalytic efficiency through a charge transfer mechanism; therefore, the Ag-CuO core-shell nanoparticles are electro-catalytically active and can induce electron-transfer reactions. The energy of a nanoparticle is dependent on the charge distribution within the energy levels of its component metal. Ultimately, the additional electrons can be discharged when glucose is introduced into the system as an electron acceptor.

This glucose oxidation mechanism can be summarised as: (1) deprotonation of glucose that causes oxidation, (2) isomerization and enediol formation, and, finally, (3) adsorption to the electrode surface, which leads to the oxidation of Cu(II)/Cu(III):



In the core-shell nanoparticle, Cu(II) was oxidised to Cu(III) and this catalysed glucose oxidation to produce gluconolactone, which was further oxidised to gluconic acid as presented in Equations (2) and (3).

4.1.3. Anticancer

Lastly, plant extract-mediated Cu-NMs have been studied for their anticancer properties. Generally, this activity can be realised through multiple routes including ROS generation, antioxidant activity, cell cycle arrest, apoptosis, and autophagy [205,207]. One study produced CuO nanoparticles using extracts of *Azadirachta indica*, *Hibiscus rosa-sinensis*, *Murraya koenigii*, *Moringa oleifera*, and *Tamarindus indica* and used MTT assays to test their activity against four cancer cell lines, i.e., human breast, cervical, epithelioma, and lung cancer cells, along with one normal human dermal fibroblast (NHDF) cell line [211]. All CuO nanoparticles exhibited anticancer ability towards all cancer cell types in a dose-dependent manner: higher concentrations of CuO nanoparticles resulted in lower cancer cell viability. Interestingly, the type of plant utilised also affected anti-cancer ability, with *Tamarindus indica*-mediated CuO nanoparticles exhibiting greater cytotoxicity over the others; this indicates that the phytochemicals in the plant extract used for nanoparticle synthesis impact the resulting particles' anti-cancer activity.

The toxicity of Cu-NMs is one of the limitations that hinder their application biomedically. However, it has been reported that plant-mediated Cu nanomaterials have less toxicity to normal human cell lines [205]. Therefore, such Cu nanomaterials may be more safely applied in biomedical applications. For example, CuO nanoparticles synthesised using extracts of *Azadirachta indica*, *Hibiscus rosa-sinensis*, *Murraya koenigii*, *Moringa oleifera*, and *Tamarindus indica* exhibited lower toxicity in NHDF cells, which suggests these to be promising anticancer agents for use in the pharmaceutical industry [211].

4.2. Environmental Remediation

The usage of Cu-NMs in environmental applications is mainly focused on the remediation of dyes and toxic compounds, with mechanisms primarily based on photocatalysis or catalysis.

The mechanism of photocatalysis by nanomaterials is as follows: when the nanomaterials are deposited into an aqueous sample containing compounds that are desired to be degraded, such as dye, and exposed to light, an interaction occurs in which a photogenerated electron is converted from the valence band (VB) to the conduction band (CB) in the nanomaterial. A hole in the VB then results, producing an electron (e^-)-hole (h^+) pair. The holes react with OH ions in the water molecules to yield OH radicals via oxidation, while the electrons react with dissolved O_2 to generate O_2 radicals via reduction. Those radicals are then responsible for the degradation of the dye into non-toxic degraded products [171,176]. Alshehri and Malik investigated the ability of *Origanum vulgare* extract-mediated Cu-Co-Ni trimetallic nanoparticles to photocatalyse the degradation of methylene blue [176]. They observed degradation efficiency of more than 50% and 92.67% after 50 and 100 min, respectively. The rate of degradation could be increased via increasing nanoparticle concentration, but after a certain threshold was surpassed, the photocatalytic efficiency could be enhanced no further due to the aggregation of the nanomaterials.

With regard to catalysis mechanisms, nanoparticles can catalyse reactions by borylation, clock reactions, oxidative coupling, A3 coupling, click chemistry, tandem and multicomponent reactions, C-H functionalization, cross-coupling, reduction and oxidation reactions, and other mixed reactions [212]. Successful catalysis via plant-mediated Cu-NMs has been achieved, such as when Suvarna et al. [173] studied the degradation of methyl green dye using bimetallic spherical Fe-Cu nanoparticles produced using *Cyclea peltata* extract, and achieved a degradation efficacy of 82% within 105 min. The Fe-Cu nanoparticles promoted hydrolysis and deprotonation reactions on the dye molecules, resulting in the demineralization of the dye molecules into simpler structures. In another example, Rosbero and Camacho utilised bimetallic (Ag and Cu) alloy nanoparticles produced via *Carica papaya* leaf extract to degrade the pesticide chlorpyrifos in water [172]. The degradation was observed for 24 h, and yielded the products

3,5,6-trichloropyridinol (TCP) and diethylthiophosphate (DETP), of which the former is less toxic than chlorpyrifos and not mutagenic.

5. Future Research Directions

Although plant-mediated Cu-NMs have numerous benefits and applications, they also have considerable potential yet to be discovered along with disadvantages that are unavoidable and need to be addressed to ensure realization of the applicability of these nanoparticles toward industrial production with wider applications. This section suggests areas of future research to increase the potential of Cu-NMs and propel the applicability of their production at a larger scale via eradicating current limitations; specifically, it discusses: (i) solutions by which to overcome limitations, (ii) potential new applications, and (iii) new research directions regarding Cu-NM synthesis.

5.1. Limitations and Solutions

This section illustrates the limitations of green Cu nanomaterial production and associated solutions. There are several that need attention in this respect, mainly with regard to biomass obtainability, the complexity of plant systems, the underlying synthesis process, nanomaterial quality, and low productivity.

Concerning bioresource accessibility, most research to date has focused on the use of local plant species that are not widely available throughout the globe; notably, variation in plant species and also geographical cultivation areas affect the phytochemicals within the plant extract produced [36]. Moreover, the inherent complexity of plants is another hindrance to the industrial production of plant-mediated Cu-NMs. That is, the phytochemicals within a plant are greatly affected by external factors such as abiotic environmental factors, cultivar, and mutagenesis [213–215]. These will cause batch-to-batch variation among raw materials, which might adversely affect the homogeneity and reproducibility of nanomaterial synthesis. On top of those considerations, another drawback to this method is the diversity of phytochemicals in a plant system. This can be addressed by applying molecular science techniques such as genetic engineering to maximize the most relevant phytochemicals in the target plant. Combining these techniques with plant-tissue culture methods such as cloning can allow the quality of a plant (target phytochemical composition and content) to be preserved and controlled and, thus, avoid batch-to-batch variation and mutagenic factors that might affect the phytochemical profile. Plant-tissue culture techniques can also minimize the time, cost, and labour force needed for the planting of bioresources and overcome geographical limitations [216].

At present, most research into plant-mediated nanoparticles is carried out in low quantities, and, hence, with low productivity. Although the quantity of nanoparticles required for characterization or application research purposes is not high, mass production via the green synthesis method is little-studied and needs to be researched in order to produce nanoparticles in a large quantity. Bioprocess methods can be used to produce and maximize specific phytochemicals for nanomaterial production and allow large-scale industrial production. With these solutions and more research, the global industrial production of uniform plant-mediated Cu nanomaterial products could be realised.

However, given the limited determinations of phytochemical profiles, it is not feasible to elucidate the mechanism of nanomaterial synthesis. This will affect the possibility of producing nanomaterials with good homogeneity in terms of size, shape, and crystal structure [71,75,79,84,217]. When it comes to investigating those phytochemicals that are responsible for stabilizing and reducing the ions within a precursor material, Fourier-transform infrared spectroscopy (FTIR) is the current technique of choice. This characterisation method mainly examines the functional groups that are deposited on the nanoparticle surface [71,79,84,177]. Although FTIR can identify the functional groups that act as stabilizing and reducing agents, it has difficulty determining which specific phytoconstituents of a complex plant extract they originated with. Further research employing other characterization methods such as liquid chromatography–mass spectrometry and

nuclear magnetic resonance can be carried out to identify the chemical structures of the contributing phytochemicals [218,219].

5.2. Potential New Applications

At present, most Cu-NMs produced via plant-mediated methods are synthesised using leaf extracts. There is plenty of room for future research into the exploitation of other plant components (peelings, roots and rhizomes, fruits, flowers, and seeds) for the synthesis of Cu alloy, core shell, and nanoparticles. In addition, there remains a knowledge gap regarding the effect of method parameters on the morphology of the synthesised particles. From an application perspective, most uses of plant-mediated Cu nanomaterials are focused on biomedical and environmental remediation. However, there are more applications that have yet to be discovered. For example, in the biological sector, research into the use of plant-mediated Cu-NMs mainly concerns their antibacterial ability and lesser antifungal ability. The relatively lower antifungal performance is owed to fungal cells less readily adsorbing nanoparticles at low concentrations as compared to bacterial cells. In addition, the binding of nanoparticles to the bacterial surface blocks bacterial respiration, whereas for fungal or eukaryotic cells, respiration occurs in the mitochondrial membrane and so is less susceptible to direct inhibition by nanoparticles [31]. There has also been limited research on the antiviral and antiparasitic abilities of plant-mediated Cu nanoparticles; further investigation in this area may expand their antimicrobial capabilities. Finally, other noble-metal (Au and Ag) nanomaterials produced via plant-mediated synthesis have been employed in other applications such as electrochemistry, detection, surface-enhanced Raman scattering, phase transfer, transmetallation, and modified glassy carbon electrodes; therefore, research can be carried out to expand the usage of Cu-NMs to these applications [31].

5.3. New Research Directions for Synthesis

One area of future research for the application of Cu-NMs and their industrial-scale green production is leveraging machine learning. Specifically, machine-learning algorithms can be used in two respects, synthetic outcome prediction and experiment planning [220]. For the first, an algorithm mathematically learns the relationship between nanomaterial properties and experimental conditions, then predicts from an example synthetic parameters dataset and the results of past experiments the characteristics of the nanoparticles that will be produced. Meanwhile, experiment-planning algorithms aim to suggest the best reaction conditions for achieving desired nanomaterial properties [220]. This can aid in reducing the time and research effort required to obtain a desired outcome, such as the uniformity of the produced particles. Most machine-learning studies to date have concentrated on chemical-based nanomaterial synthesis; only a limited number of publications have concerned green synthesis; hence, there remains a large gap in this area [221–224]. Addressing this gap can help in making the process of Cu nanomaterial synthesis become less labour intensive, more cost effective, less time consuming, more productive, and able to yield higher quality nanoparticles, all of which are important from the industrial perspective.

6. Conclusions

This literature review focused on the green synthesis of Cu nanomaterials. Compared to chemical or physical synthesis methods, green synthesis and especially plant-mediated synthesis is more environment-friendly, less toxic, and safe throughout the whole production process. The production methodology was discussed with further focus on plant-mediated nanomaterial synthesis, including the plant extraction method and Cu-NM (pure metal, metal oxide, alloy, core shell, and nanoparticles) synthesis. Leaf-extract-mediated Cu nanomaterials comprise the majority produced to date, with few synthesised using other types of plant components. The review also considered the biological and environmental applications of plant-mediated Cu-NMs. With regard to biological applications, antiviral and antiparasitic activities have received less focus than antibacterial. There also remain many research gaps regarding the

application of green synthesis Cu-NMs in other sectors. Finally, current limitations and solutions with potential future research targets were described. Biomass obtainability, complexity of plant systems, underlying synthesis process, nano-material quality, and low productivity are the future challenges that need to be addressed in order to further broaden the application of plant-mediated nanomaterial synthesis.

In short, plant-mediated nanomaterial synthesis is eco-friendly, has low toxicity, and avoids using hazardous chemicals. The process can be separated into two parts, the plant extraction and the nanomaterial production. Different plant extracts with different parameters can produce nanomaterials of different sizes and geometries. As such, plant source accessibility, diversity of phytochemicals in extracts, knowledge of the synthesis mechanism, and nanomaterial quality are the limitations that presently hinder the future industrial production and application of plant-mediated nanomaterials. More research is needed in areas of the biotechnological sector such as phytochemical profiling, molecular science, tissue culture, and bioprocesses to overcome these issues. Separately, machine learning can also be adopted as a new research topic to further improve the green synthesis of Cu-NMs with better industrial applicability. Once these problems and research directions are resolved and fulfilled, respectively, the potential of plant-mediated nanomaterial synthesis could be fully unleashed in myriad applications, providing processes and materials with better sustainability and friendliness toward the environment.

Author Contributions: Investigation, writing—original draft, J.V.; Conceptualization, writing—review and editing, K.S.L.; Supervision, visualization, Y.C.-Y.E.; Funding acquisition, validation, S.X.C.; Supervision, validation, M.S.; Conceptualization, supervision, writing—review and editing, C.H.C. All authors have read and agreed to the published version of the manuscript.

Funding: This research was funded by the Center for Research and Instrumentation Management (CRIM), Universiti Kebangsaan Malaysia, grant number FRGS/1/2019/STG01/UKM/02/11.

Data Availability Statement: Not applicable.

Acknowledgments: Not applicable.

Conflicts of Interest: The authors declare no conflict of interest. The funders had no role in the design of the study; in the collection, analyses, or interpretation of data; in the writing of the manuscript; or in the decision to publish the results.

References

1. Coffin, J.D.; Rao, R.; Lurie, D.I. Translational Potential of Ayurveda Prakriti: Concepts in the Area of Personalized Medicine. In *Translational Ayurveda*; Springer: Singapore, 2019; pp. 21–32.
2. Liu, W.; Lu, L.; Ma, C.; Yan, C.; Zhao, Z.; Mohammadtursun, N.; Hu, L.; Tulake, W.; Jiang, S.; Gao, Z.; et al. The Evolution of Traditional Chinese Medicine as a Disciplinary Concept and Its Essence throughout History. *Tradit. Med. Mod. Med.* **2018**, *01*, 171–180. [[CrossRef](#)]
3. Wang, J.; Wong, Y.-K.; Liao, F. What Has Traditional Chinese Medicine Delivered for Modern Medicine? *Expert Rev. Mol. Med.* **2018**, *20*, e4. [[CrossRef](#)] [[PubMed](#)]
4. Zhang, Q.-W.; Lin, L.-G.; Ye, W.-C. Techniques for Extraction and Isolation of Natural Products: A Comprehensive Review. *Chin. Med.* **2018**, *13*, 20. [[CrossRef](#)] [[PubMed](#)]
5. Jiang, S.; Wang, M.; Jiang, L.; Xie, Q.; Yuan, H.; Yang, Y.; Zafar, S.; Liu, Y.; Jian, Y.; Li, B.; et al. The Medicinal Uses of the Genus *Bletilla* in Traditional Chinese Medicine: A Phytochemical and Pharmacological Review. *J. Ethnopharmacol.* **2021**, *280*, 114263. [[CrossRef](#)]
6. Nille, G.C.; Chaudhary, A.K. Potential Implications of Ayurveda in Psoriasis: A Clinical Case Study. *J. Ayurveda Integr. Med.* **2021**, *12*, 172–177. [[CrossRef](#)] [[PubMed](#)]
7. Hu, Y.; Zhai, W.; Chen, H.; Li, L.; Gao, W.; Wei, Y.; Wu, J. Current Understanding of Phytochemicals from Chinese Herbal Medicines for Ferroptosis-Mediated Cancer Prevention and Treatment. *Pharmacol. Res. Mod. Chin. Med.* **2022**, *3*, 100100. [[CrossRef](#)]
8. Ekiert, H.; Pajor, J.; Klin, P.; Rzepiela, A.; Ślesak, H.; Szopa, A. Significance of *Artemisia vulgaris* L. (Common Mugwort) in the History of Medicine and Its Possible Contemporary Applications Substantiated by Phytochemical and Pharmacological Studies. *Molecules* **2020**, *25*, 4415. [[CrossRef](#)]
9. Dubey, S.P.; Lahtinen, M.; Sillanpää, M. Green Synthesis and Characterizations of Silver and Gold Nanoparticles Using Leaf Extract of *Rosa rugosa*. *Colloids Surf. A Physicochem. Eng. Asp.* **2010**, *364*, 34–41. [[CrossRef](#)]

10. Dubey, S.P.; Lahtinen, M.; Sillanpää, M. Tansy Fruit Mediated Greener Synthesis of Silver and Gold Nanoparticles. *Process Biochem.* **2010**, *45*, 1065–1071. [[CrossRef](#)]
11. Jadoun, S.; Arif, R.; Jangid, N.K.; Meena, R.K. Green Synthesis of Nanoparticles Using Plant Extracts: A Review. *Environ. Chem. Lett.* **2021**, *19*, 355–374. [[CrossRef](#)]
12. Azri, F.A.; Selamat, J.; Sukor, R.; Yusof, N.A.; Raston, N.H.A.; Nordin, N.; Jambari, N.N. Etlingera Elatior-Mediated Synthesis of Gold Nanoparticles and Their Application as Electrochemical Current Enhancer. *Molecules* **2019**, *24*, 3141. [[CrossRef](#)]
13. Pal, G.; Rai, P.; Pandey, A. Green Synthesis of Nanoparticles: A Greener Approach for a Cleaner Future. In *Green Synthesis, Characterization and Applications of Nanoparticles*; Elsevier: Amsterdam, The Netherlands, 2019; pp. 1–26.
14. Waris, A.; Din, M.; Ali, A.; Ali, M.; Afridi, S.; Baset, A.; Ullah Khan, A. A Comprehensive Review of Green Synthesis of Copper Oxide Nanoparticles and Their Diverse Biomedical Applications. *Inorg. Chem. Commun.* **2021**, *123*, 108369. [[CrossRef](#)]
15. Jusoh, R.; Kamarudin, N.H.N.; Kamarudin, N.S.; Sukor, N.F. Green Synthesis of Spherical Shaped Silver Nanoparticles Using *Allium cepa* Leaves Extract and Its Photocatalytic Activity. *Mater. Sci. Forum* **2019**, *962*, 57–62. [[CrossRef](#)]
16. Md Ishak, N.A.I.; Kamarudin, S.K.; Timmiati, S.N. Green Synthesis of Metal and Metal Oxide Nanoparticles via Plant Extracts: An Overview. *Mater. Res. Express* **2019**, *6*, 112004. [[CrossRef](#)]
17. Chin, P.P.; Ding, J.; Yi, J.B.; Liu, B.H. Synthesis of FeS₂ and FeS Nanoparticles by High-Energy Mechanical Milling and Mechanochemical Processing. *J. Alloys Compd.* **2005**, *390*, 255–260. [[CrossRef](#)]
18. De Carvalho, J.F.; De Medeiros, S.N.; Morales, M.A.; Dantas, A.L.; Carriço, A.S. Synthesis of Magnetite Nanoparticles by High Energy Ball Milling. *Appl. Surf. Sci.* **2013**, *275*, 84–87. [[CrossRef](#)]
19. Prabhu, S.; Poulose, E.K. Silver Nanoparticles: Mechanism of Antimicrobial Action, Synthesis, Medical Applications, and Toxicity Effects. *Int. Nano-Lett.* **2012**, *2*, 32. [[CrossRef](#)]
20. Seino, S.; Kinoshita, T.; Nakagawa, T.; Kojima, T.; Taniguchi, R.; Okuda, S.; Yamamoto, T.A. Radiation Induced Synthesis of Gold/Iron-Oxide Composite Nanoparticles Using High-Energy Electron Beam. *J. Nanopart. Res.* **2008**, *10*, 1071–1076. [[CrossRef](#)]
21. Agarwal, H.; Nakara, A.; Shanmugam, V.K. Anti-Inflammatory Mechanism of Various Metal and Metal Oxide Nanoparticles Synthesized Using Plant Extracts: A Review. *Biomed. Pharmacother.* **2019**, *109*, 2561–2572. [[CrossRef](#)]
22. Iravani, S. Green Synthesis of Metal Nanoparticles Using Plants. *Green Chem.* **2011**, *13*, 2638–2650. [[CrossRef](#)]
23. Kumaran, A.; Joel Karunakaran, R. In Vitro Antioxidant Activities of Methanol Extracts of Five Phyllanthus Species from India. *LWT Food Sci. Technol.* **2007**, *40*, 344–352. [[CrossRef](#)]
24. Lu, F.; Sun, D.; Huang, J.; Du, M.; Yang, F.; Chen, H.; Hong, Y.; Li, Q. Plant-Mediated Synthesis of Ag-Pd Alloy Nanoparticles and Their Application as Catalyst toward Selective Hydrogenation. *ACS Sustain. Chem. Eng.* **2014**, *2*, 1212–1218. [[CrossRef](#)]
25. Madhubala, V.; Kalaivani, T. Phyto and Hydrothermal Synthesis of Fe₃O₄@ZnO Core-Shell Nanoparticles Using *Azadirachta indica* and Its Cytotoxicity Studies. *Appl. Surf. Sci.* **2018**, *449*, 584–590. [[CrossRef](#)]
26. Phang, Y.K.; Aminuzzaman, M.; Akhtaruzzaman, M.; Muhammad, G.; Ogawa, S.; Watanabe, A.; Tey, L.H. Green Synthesis and Characterization of CuO Nanoparticles Derived from Papaya Peel Extract for the Photocatalytic Degradation of Palm Oil Mill Effluent (POME). *Sustainability* **2021**, *13*, 796. [[CrossRef](#)]
27. Selvanathan, V.; Aminuzzaman, M.; Tey, L.H.; Razali, S.A.; Althubeiti, K.; Alkhamash, H.I.; Guha, S.K.; Ogawa, S.; Watanabe, A.; Shahiduzzaman, M.; et al. Muntingia Calabura Leaves Mediated Green Synthesis of CuO Nanorods: Exploiting Phytochemicals for Unique Morphology. *Materials* **2021**, *14*, 6379. [[CrossRef](#)]
28. Karim, N.A.; Rubinsin, N.J.; Burukan, M.A.A.; Kamarudin, S.K. Sustainable Route of Synthesis Platinum Nanoparticles Using Orange Peel Extract. *Int. J. Green Energy* **2019**, *16*, 1518–1526. [[CrossRef](#)]
29. Ali, A.; Sattar, M.; Hussain, F.; Tareen, M.H.K.; Militky, J.; Noman, M.T. Single-step Green Synthesis of Highly Concentrated and Stable Colloidal Dispersion of Core-shell Silver Nanoparticles and Their Antimicrobial and Ultra-high Catalytic Properties. *Nanomaterials* **2021**, *11*, 1007. [[CrossRef](#)]
30. Villalobos-Noriega, J.M.A.; Rodríguez-León, E.; Rodríguez-Beas, C.; Larios-Rodríguez, E.; Plascencia-Jatomea, M.; Martínez-Higuera, A.; Acuña-Campa, H.; García-Galaz, A.; Mora-Monroy, R.; Alvarez-Cirerol, F.J.; et al. Au@Ag Core@Shell Nanoparticles Synthesized with Rumex Hymenosepalus as Antimicrobial Agent. *Nanoscale Res. Lett.* **2021**, *16*, 118. [[CrossRef](#)]
31. Dauthal, P.; Mukhopadhyay, M. Noble Metal Nanoparticles: Plant-Mediated Synthesis, Mechanistic Aspects of Synthesis, and Applications. *Ind. Eng. Chem. Res.* **2016**, *55*, 9557–9577. [[CrossRef](#)]
32. Andra, S.; Balu, S.K.; Jeevanandham, J.; Muthalagu, M.; Vidyavathy, M.; Chan, Y.S.; Danquah, M.K. Phytosynthesized Metal Oxide Nanoparticles for Pharmaceutical Applications. *Naunyn Schmiedeberg's Arch. Pharmacol.* **2019**, *392*, 755–771. [[CrossRef](#)]
33. Annu, A.A.; Ahmed, S. Green Synthesis of Metal, Metal Oxide Nanoparticles, and Their Various Applications. In *Handbook of Ecomaterials*; Springer International Publishing: Cham, Switzerland, 2018; pp. 1–45.
34. Song, X.R.; Yu, S.X.; Jin, G.X.; Wang, X.; Chen, J.; Li, J.; Liu, G.; Yang, H.H. Plant Polyphenol-Assisted Green Synthesis of Hollow CoPt Alloy Nanoparticles for Dual-Modality Imaging Guided Photothermal Therapy. *Small* **2016**, *12*, 1506–1513. [[CrossRef](#)] [[PubMed](#)]
35. Chowdhury, R.; Mollick, M.M.R.; Biswas, Y.; Chattopadhyay, D.; Rashid, M.H. Biogenic Synthesis of Shape-Tunable Au-Pd Alloy Nanoparticles with Enhanced Catalytic Activities. *J. Alloys Compd.* **2018**, *763*, 399–408. [[CrossRef](#)]
36. Ying, S.; Guan, Z.; Ofoegbu, P.C.; Clubb, P.; Rico, C.; He, F.; Hong, J. Green Synthesis of Nanoparticles: Current Developments and Limitations. *Environ. Technol. Innov.* **2022**, *26*, 102336. [[CrossRef](#)]

37. Mutalik, C.; Okoro, G.; Krisnawati, D.I.; Jazidie, A.; Rahmawati, E.Q.; Rahayu, D.; Hsu, W.-T.; Kuo, T.-R. Copper Sulfide with Morphology-Dependent Photodynamic and Photothermal Antibacterial Activities. *J. Colloid Interface Sci.* **2022**, *607*, 1825–1835. [[CrossRef](#)] [[PubMed](#)]
38. Guo, H.; Lin, N.; Chen, Y.; Wang, Z.; Xie, Q.; Zheng, T.; Gao, N.; Li, S.; Kang, J.; Cai, D.; et al. Copper Nanowires as Fully Transparent Conductive Electrodes. *Sci. Rep.* **2013**, *3*, 2323. [[CrossRef](#)]
39. Hashimi, A.S.; Ginting, R.T.; Chin, S.X.; Lau, K.S.; Nazhif Mohd Nohan, M.A.; Zakaria, S.; Yap, C.C.; Chia, C.H. Fast Microwave-Assisted Synthesis of Copper Nanowires as Reusable High-Performance Transparent Conductive Electrode. *Curr. Appl. Phys.* **2020**, *20*, 205–211. [[CrossRef](#)]
40. Jin, M.; He, G.; Zhang, H.; Zeng, J.; Xie, Z.; Xia, Y. Shape-Controlled Synthesis of Copper Nanocrystals in an Aqueous Solution with Glucose as a Reducing Agent and Hexadecylamine as a Capping Agent. *Angew. Chem. Int. Ed.* **2011**, *50*, 10560–10564. [[CrossRef](#)]
41. Rathmell, A.R.; Wiley, B.J. The Synthesis and Coating of Long, Thin Copper Nanowires to Make Flexible, Transparent Conducting Films on Plastic Substrates. *Adv. Mater.* **2011**, *23*, 4798–4803. [[CrossRef](#)]
42. Ingle, A.P.; Duran, N.; Rai, M. Bioactivity, Mechanism of Action, and Cytotoxicity of Copper-Based Nanoparticles: A Review. *Appl. Microbiol. Biotechnol.* **2014**, *98*, 1001–1009. [[CrossRef](#)]
43. Jeong, S.; Woo, K.; Kim, D.; Lim, S.; Kim, J.S.; Shin, H.; Xia, Y.; Moon, J. Controlling the Thickness of the Surface Oxide Layer on Cu Nanoparticles for the Fabrication of Conductive Structures by Ink-Jet Printing. *Adv. Funct. Mater.* **2008**, *18*, 679–686. [[CrossRef](#)]
44. Christian, P.; Von Der Kammer, F.; Baalousha, M.; Hofmann, T. Nanoparticles: Structure, Properties, Preparation and Behaviour in Environmental Media. *Ecotoxicology* **2008**, *17*, 326–343. [[CrossRef](#)] [[PubMed](#)]
45. Abid, N.; Khan, A.M.; Shujait, S.; Chaudhary, K.; Ikram, M.; Imran, M.; Haider, J.; Khan, M.; Khan, Q.; Maqbool, M. Synthesis of Nanomaterials Using Various Top-down and Bottom-up Approaches, Influencing Factors, Advantages, and Disadvantages: A Review. *Adv. Colloid Interface Sci.* **2022**, *300*, 102597. [[CrossRef](#)] [[PubMed](#)]
46. Jamkhande, P.G.; Ghule, N.W.; Bamer, A.H.; Kalaskar, M.G. Metal Nanoparticles Synthesis: An Overview on Methods of Preparation, Advantages and Disadvantages, and Applications. *J. Drug Deliv. Sci. Technol.* **2019**, *53*, 101174. [[CrossRef](#)]
47. Sopicka-Lizer, M. (Ed.) *High Energy Ball Milling*; Woodhead Publishing Ltd.: Cambridge, UK, 2010; ISBN 9781845692704.
48. Rane, A.V.; Kanny, K.; Abitha, V.K.; Thomas, S. Methods for Synthesis of Nanoparticles and Fabrication of Nanocomposites. In *Synthesis of Inorganic Nanomaterials*; Woodhead Publishing Ltd.: Cambridge, UK, 2018; pp. 121–139. [[CrossRef](#)]
49. Hasanpoor, M.; Aliofkhaezraei, M.; Delavari, H. Microwave-Assisted Synthesis of Zinc Oxide Nanoparticles. *Procedia Mater. Sci.* **2015**, *11*, 320–325. [[CrossRef](#)]
50. Horwat, D.; Zakharov, D.I.; Endrino, J.L.; Soldera, F.; Anders, A.; Migot, S.; Karoum, R.; Vernoux, P.; Pierson, J.F. Chemistry, Phase Formation, and Catalytic Activity of Thin Palladium-Containing Oxide Films Synthesized by Plasma-Assisted Physical Vapor Deposition. *Surf. Coat. Technol.* **2011**, *205*, S171–S177. [[CrossRef](#)]
51. Shende, S.; Ingle, A.P.; Gade, A.; Rai, M. Green Synthesis of Copper Nanoparticles by *Citrus medica* Linn. (Idilimbu) Juice and Its Antimicrobial Activity. *World J. Microbiol. Biotechnol.* **2015**, *31*, 865–873. [[CrossRef](#)] [[PubMed](#)]
52. Machado, S.; Pacheco, J.G.; Nouws, H.P.A.; Albergaria, J.T.; Delerue-Matos, C. Characterization of Green Zero-Valent Iron Nanoparticles Produced with Tree Leaf Extracts. *Sci. Total Environ.* **2015**, *533*, 76–81. [[CrossRef](#)] [[PubMed](#)]
53. Kataria, N.; Garg, V.K. *Green Synthesis of Fe₃O₄ Nanoparticles Loaded Sawdust Carbon for Cadmium (II) Removal from Water: Regeneration and Mechanism*; Elsevier: Amsterdam, The Netherlands, 2018; Volume 208, ISBN 9198120581.
54. Pantidos, N. Biological Synthesis of Metallic Nanoparticles by Bacteria, Fungi and Plants. *J. Nanomed. Nanotechnol.* **2014**, *5*, 233. [[CrossRef](#)]
55. Nies, D.H. Microbial Heavy-Metal Resistance. *Appl. Microbiol. Biotechnol.* **1999**, *51*, 730–750. [[CrossRef](#)]
56. Silver, S. Bacterial Heavy Metal Resistance Systems and Possibility of Bioremediation. In *Biotechnology: Bridging Research and Applications*; Springer: Dordrecht, The Netherlands, 1991; pp. 265–287.
57. Guilger-Casagrande, M.; Lima, R. de Synthesis of Silver Nanoparticles Mediated by Fungi: A Review. *Front. Bioeng. Biotechnol.* **2019**, *7*, 287. [[CrossRef](#)]
58. El-Sayed, E.S.R.; Mousa, S.A.; Abdou, D.A.M.; Abo El-Seoud, M.A.; Elmehlawy, A.A.; Mohamed, S.S. Exploiting the Exceptional Biosynthetic Potency of the Endophytic *Aspergillus terreus* in Enhancing Production of Co₃O₄, CuO, Fe₃O₄, NiO, and ZnO Nanoparticles Using Bioprocess Optimization and Gamma Irradiation. *Saudi J. Biol. Sci.* **2021**, *29*, 2463–2474. [[CrossRef](#)] [[PubMed](#)]
59. Alghuthaymi, M.A.; Almoammar, H.; Rai, M.; Said-Galiev, E.; Abd-Elsalam, K.A. Myconanoparticles: Synthesis and Their Role in Phytopathogens Management. *Biotechnol. Biotechnol. Equip.* **2015**, *29*, 221–236. [[CrossRef](#)] [[PubMed](#)]
60. Khanna, P.; Kaur, A.; Goyal, D. Algae-Based Metallic Nanoparticles: Synthesis, Characterization and Applications. *J. Microbiol. Methods* **2019**, *163*, 105656. [[CrossRef](#)] [[PubMed](#)]
61. Mahmood, Q.; Mirza, N.; Shaheen, S. Phytoremediation Using Algae and Macrophytes: I. In *Phytoremediation: Management of Environmental Contaminants, Volume 2*; Springer International Publishing: Cham, Switzerland, 2015; pp. 265–289. ISBN 9783319109695.
62. Khan, F.; Shahid, A.; Zhu, H.; Wang, N.; Javed, M.R.; Ahmad, N.; Xu, J.; Alam, M.A.; Mehmood, M.A. Prospects of Algae-Based Green Synthesis of Nanoparticles for Environmental Applications. *Chemosphere* **2022**, *293*, 133571. [[CrossRef](#)]
63. Sharma, D.; Kanchi, S.; Bisetty, K. Biogenic Synthesis of Nanoparticles: A Review. *Arab. J. Chem.* **2019**, *12*, 3576–3600. [[CrossRef](#)]

64. Verma, N.; Kumar, N. Synthesis and Biomedical Applications of Copper Oxide Nanoparticles: An Expanding Horizon. *ACS Biomater. Sci. Eng.* **2019**, *5*, 1170–1188. [[CrossRef](#)]
65. Nagar, N.; Devra, V. Green Synthesis and Characterization of Copper Nanoparticles Using *Azadirachta indica* Leaves. *Mater. Chem. Phys.* **2018**, *213*, 44–51. [[CrossRef](#)]
66. Mani, M.; Pavithra, S.; Mohanraj, K.; Kumaresan, S.; Alotaibi, S.S.; Eraqi, M.M.; Gandhi, A.D.; Babujanathanam, R.; Maaza, M.; Kaviyarasu, K. Studies on the Spectrometric Analysis of Metallic Silver Nanoparticles (Ag NPs) Using *Basella alba* Leaf for the Antibacterial Activities. *Environ. Res.* **2021**, *199*, 111274. [[CrossRef](#)]
67. Zhang, G.; Du, M.; Li, Q.; Li, X.; Huang, J.; Jiang, X.; Sun, D. Green Synthesis of Au-Ag Alloy Nanoparticles Using *Cacumen platycladi* Extract. *RSC Adv.* **2013**, *3*, 1878–1884. [[CrossRef](#)]
68. Dulta, K.; Ağçeli, G.K.; Chauhan, P.; Chauhan, P.K. Biogenic Production and Characterization of CuO Nanoparticles by Carica Papaya Leaves and Its Biocompatibility Applications. *J. Inorg. Organomet. Polym. Mater.* **2021**, *31*, 1846–1857. [[CrossRef](#)]
69. Irum, S.; Jabeen, N.; Ahmad, K.S.; Shafique, S.; Khan, T.F.; Gul, H.; Anwaar, S.; Shah, N.I.; Mehmood, A.; Hussain, S.Z. Biogenic Iron Oxide Nanoparticles Enhance Callogenesis and Regeneration Pattern of Recalcitrant *Cicer arietinum* L. *PLoS ONE* **2020**, *15*, e0242829. [[CrossRef](#)] [[PubMed](#)]
70. Beheshtkhoo, N.; Kouhbanani, M.A.J.; Savardashtaki, A.; Amani, A.M.; Taghizadeh, S. Green Synthesis of Iron Oxide Nanoparticles by Aqueous Leaf Extract of *Daphne Mezereum* as a Novel Dye Removing Material. *Appl. Phys. A Mater. Sci. Process.* **2018**, *124*, 363. [[CrossRef](#)]
71. Chung, I.; Rahuman, A.A.; Marimuthu, S.; Kirthi, A.V.; Anbarasan, K.; Padmini, P.; Rajakumar, G. Green Synthesis of Copper Nanoparticles Using *Eclipta prostrata* Leaves Extract and Their Antioxidant and Cytotoxic Activities. *Exp. Ther. Med.* **2017**, *14*, 18–24. [[CrossRef](#)] [[PubMed](#)]
72. Bhat, M.; Chakraborty, B.; Kumar, R.S.; Almansour, A.I.; Arumugam, N.; Kotresha, D.; Pallavi, S.S.; Dhanyakumara, S.B.; Shashiraj, K.N.; Nayaka, S. Biogenic Synthesis, Characterization and Antimicrobial Activity of *Ixora Brachypoda* (DC) Leaf Extract Mediated Silver Nanoparticles. *J. King Saud Univ. Sci.* **2021**, *33*, 101296. [[CrossRef](#)]
73. Dipankar, C.; Murugan, S. The Green Synthesis, Characterization and Evaluation of the Biological Activities of Silver Nanoparticles Synthesized from *Iresine Herbstii* Leaf Aqueous Extracts. *Colloids Surf. B Biointerfaces* **2012**, *98*, 112–119. [[CrossRef](#)] [[PubMed](#)]
74. Yallappa, S.; Manjanna, J.; Dhananjaya, B.L. Phytosynthesis of Stable Au, Ag and Au-Ag Alloy Nanoparticles Using *J. Sambac* Leaves Extract, and Their Enhanced Antimicrobial Activity in Presence of Organic Antimicrobials. *Spectrochim. Acta Part A Mol. Biomol. Spectrosc.* **2015**, *137*, 236–243. [[CrossRef](#)]
75. Lee, H.J.; Song, J.Y.; Kim, B.S. Biological Synthesis of Copper Nanoparticles Using *Magnolia kobus* Leaf Extract and Their Antibacterial Activity. *J. Chem. Technol. Biotechnol.* **2013**, *88*, 1971–1977. [[CrossRef](#)]
76. Nouri, A.; Tavakkoli Yarak, M.; Lajevardi, A.; Rezaei, Z.; Ghorbanpour, M.; Tanzifi, M. Ultrasonic-Assisted Green Synthesis of Silver Nanoparticles Using *Mentha aquatica* Leaf Extract for Enhanced Antibacterial Properties and Catalytic Activity. *Colloids Interface Sci. Commun.* **2020**, *35*, 100252. [[CrossRef](#)]
77. Boruah, J.S.; Devi, C.; Hazarika, U.; Bhaskar Reddy, P.V.; Chowdhury, D.; Barthakur, M.; Kalita, P. Green Synthesis of Gold Nanoparticles Using an Antiepileptic Plant Extract: In Vitro Biological and Photo-Catalytic Activities. *RSC Adv.* **2021**, *11*, 28029–28041. [[CrossRef](#)]
78. Usha Rani, P.; Rajasekharreddy, P. Green Synthesis of Silver-Protein (Core-Shell) Nanoparticles Using *Piper betle* L. Leaf Extract and Its Ecotoxicological Studies on *Daphnia Magna*. *Colloids Surf. A Physicochem. Eng. Asp.* **2011**, *389*, 188–194. [[CrossRef](#)]
79. Nasrollahzadeh, M.; Momeni, S.S.; Sajadi, S.M. Green Synthesis of Copper Nanoparticles Using *Plantago asiatica* Leaf Extract and Their Application for the Cyanation of Aldehydes Using $K_4Fe(CN)_6$. *J. Colloid Interface Sci.* **2017**, *506*, 471–477. [[CrossRef](#)] [[PubMed](#)]
80. Kocadag Kocazorbaz, E.; Moulahoum, H.; Tut, E.; Sarac, A.; Tok, K.; Yalcin, H.T.; Zihnioglu, F. Kermes Oak (*Quercus coccifera* L.) Extract for a Biogenic and Eco-Benign Synthesis of Silver Nanoparticles with Efficient Biological Activities. *Environ. Technol. Innov.* **2021**, *24*, 102067. [[CrossRef](#)]
81. Vasantharaj, S.; Sathiyavimal, S.; Senthilkumar, P.; LewisOscar, F.; Pugazhendhi, A. Biosynthesis of Iron Oxide Nanoparticles Using Leaf Extract of *Ruellia tuberosa*: Antimicrobial Properties and Their Applications in Photocatalytic Degradation. *J. Photochem. Photobiol. B Biol.* **2019**, *192*, 74–82. [[CrossRef](#)] [[PubMed](#)]
82. Elemike, E.E.; Onwudiwe, D.C.; Fayemi, O.E.; Botha, T.L. Green Synthesis and Electrochemistry of Ag, Au, and Ag–Au Bimetallic Nanoparticles Using Golden Rod (*Solidago canadensis*) Leaf Extract. *Appl. Phys. A Mater. Sci. Process.* **2019**, *125*, 42. [[CrossRef](#)]
83. Sadiq, H.; Sher, F.; Sehar, S.; Lima, E.C.; Zhang, S.; Iqbal, H.M.N.; Zafar, F.; Nuhanović, M. Green Synthesis of ZnO Nanoparticles from *Syzygium Cumini* Leaves Extract with Robust Photocatalysis Applications. *J. Mol. Liq.* **2021**, *335*, 116567. [[CrossRef](#)]
84. Sivaraj, R.; Rahman, P.K.S.M.; Rajiv, P.; Salam, H.A.; Venkatesh, R. Biogenic Copper Oxide Nanoparticles Synthesis Using *Tabernaemontana divaricate* Leaf Extract and Its Antibacterial Activity against Urinary Tract Pathogen. *Spectrochim. Acta Part A Mol. Biomol. Spectrosc.* **2014**, *133*, 178–181. [[CrossRef](#)]
85. Nasrollahzadeh, M.; Sajadi, S.M.; Rostami-Vartooni, A.; Hussin, S.M. Green Synthesis of CuO Nanoparticles Using Aqueous Extract of *Thymus vulgaris* L. Leaves and Their Catalytic Performance for N-Arylation of Indoles and Amines. *J. Colloid Interface Sci.* **2016**, *466*, 113–119. [[CrossRef](#)]

86. Le, N.T.T.; Thi, T.T.H.; Ching, Y.C.; Nguyen, N.H.; Nguyen, D.Y.P.; Truong, Q.M.; Nguyen, D.H. Garcinia Mangostana Shell and Tradescantia Spathacea Leaf Extract-Mediated One-Pot Synthesis of Silver Nanoparticles with Effective Antifungal Properties. *Curr. Nanosci.* **2020**, *17*, 762–771. [[CrossRef](#)]
87. Martínez-cabanas, M.; López-garcía, M.; Rodríguez-barro, P.; Vilariño, T.; Lodeiro, P.; Herrero, R.; Barriada, J.L.; de Vicente, M.E.S. Antioxidant Capacity Assessment of Plant Extracts for Green Synthesis of Nanoparticles. *Nanomaterials* **2021**, *11*, 1679. [[CrossRef](#)]
88. Nasrollahzadeh, M.; Maham, M.; Rostami-Vartooni, A.; Bagherzadeh, M.; Sajadi, S.M. Barberry Fruit Extract Assisted in Situ Green Synthesis of Cu Nanoparticles Supported on a Reduced Graphene Oxide-Fe₃O₄ Nanocomposite as a Magnetically Separable and Reusable Catalyst for the O-Arylation of Phenols with Aryl Halides under Ligand-Free Cond. *RSC Adv.* **2015**, *5*, 64769–64780. [[CrossRef](#)]
89. Zarei, M.; Seyedi, N.; Maghsoudi, S.; Nejad, M.S.; Sheibani, H. Green Synthesis of Ag Nanoparticles on the Modified Graphene Oxide Using *Capparis spinosa* Fruit Extract for Catalytic Reduction of Organic Dyes. *Inorg. Chem. Commun.* **2021**, *123*, 108327. [[CrossRef](#)]
90. Jahan, I.; Erci, F.; Isildak, I. Facile Microwave-Mediated Green Synthesis of Non-Toxic Copper Nanoparticles Using *Citrus sinensis* Aqueous Fruit Extract and Their Antibacterial Potentials. *J. Drug Deliv. Sci. Technol.* **2021**, *61*, 102172. [[CrossRef](#)]
91. Lakshmanan, G.; Sathiyaseelan, A.; Kalaichelvan, P.T.; Murugesan, K. Plant-Mediated Synthesis of Silver Nanoparticles Using Fruit Extract of *Cleome viscosa* L.: Assessment of Their Antibacterial and Anticancer Activity. *Karbala Int. J. Mod. Sci.* **2018**, *4*, 61–68. [[CrossRef](#)]
92. Sathishkumar, G.; Logeshwaran, V.; Sarathbabu, S.; Jha, P.K.; Jeyaraj, M.; Rajkuberan, C.; Senthilkumar, N.; Sivaramakrishnan, S. Green Synthesis of Magnetic Fe₃O₄ Nanoparticles Using *Couroupita guianensis* Aubl. Fruit Extract for Their Antibacterial and Cytotoxicity Activities. *Artif. Cells Nanomed. Biotechnol.* **2018**, *46*, 589–598. [[CrossRef](#)] [[PubMed](#)]
93. Ebrahimzadeh, M.A.; Mortazavi-Derazkola, S.; Zazouli, M.A. Eco-Friendly Green Synthesis and Characterization of Novel Fe₃O₄/SiO₂/Cu₂O–Ag Nanocomposites Using *Crataegus pentagyna* Fruit Extract for Photocatalytic Degradation of Organic Contaminants. *J. Mater. Sci. Mater. Electron.* **2019**, *30*, 10994–11004. [[CrossRef](#)]
94. Ramesh, P.S.; Kokila, T.; Geetha, D. Plant Mediated Green Synthesis and Antibacterial Activity of Silver Nanoparticles Using *Emblia officinalis* Fruit Extract. *Spectrochim. Acta Part A Mol. Biomol. Spectrosc.* **2015**, *142*, 339–343. [[CrossRef](#)]
95. Aksu Demirezen, D.; Yıldız, Y.Ş.; Yılmaz, Ş.; Demirezen Yılmaz, D. Green Synthesis and Characterization of Iron Oxide Nanoparticles Using *Ficus carica* (Common Fig) Dried Fruit Extract. *J. Biosci. Bioeng.* **2019**, *127*, 241–245. [[CrossRef](#)] [[PubMed](#)]
96. Sun, L.; Yin, Y.; Lv, P.; Su, W.; Zhang, L. Green Controllable Synthesis of Au-Ag Alloy Nanoparticles Using Chinese Wolfberry Fruit Extract and Their Tunable Photocatalytic Activity. *RSC Adv.* **2018**, *8*, 3964–3973. [[CrossRef](#)]
97. Nasrollahzadeh, M.; Mohammad Sajadi, S.; Maham, M.; Ehsani, A. Facile and Surfactant-Free Synthesis of Pd Nanoparticles by the Extract of the Fruits of Piper Longum and Their Catalytic Performance for the Sonogashira Coupling Reaction in Water under Ligand- and Copper-Free Conditions. *RSC Adv.* **2015**, *5*, 2562–2567. [[CrossRef](#)]
98. Veeramani, C.; Newehy, A.S.E.; Alsaif, M.A.; Al-Numair, K.S. Pouteria Caimito Nutritional Fruit Derived Silver Nanoparticles and Core-Shell Nanospheres Synthesis, Characterization, and Their Oral Cancer Preventive Efficiency. *J. Mol. Struct.* **2021**, *1245*, 131227. [[CrossRef](#)]
99. Chelli, V.R.; Golder, A.K. One Pot Green Synthesis of Pt, Co and Pt@Co Core-Shell Nanoparticles Using *Sechium edule*. *J. Chem. Technol. Biotechnol.* **2019**, *94*, 911–918. [[CrossRef](#)]
100. Pilaquinga, F.; Morejón, B.; Ganchala, D.; Morey, J.; Piña, N.; Debut, A.; Neira, M. Green Synthesis of Silver Nanoparticles Using *Solanum mammosum* L. (Solanaceae) Fruit Extract and Their Larvicidal Activity against *Aedes aegypti* L. (Diptera: Culicidae). *PLoS ONE* **2019**, *14*, e0224109. [[CrossRef](#)] [[PubMed](#)]
101. Yugandhar, P.; Vasavi, T.; Jayavardhana Rao, Y.; Uma Maheswari Devi, P.; Narasimha, G.; Savithamma, N. Cost Effective, Green Synthesis of Copper Oxide Nanoparticles Using Fruit Extract of *Syzygium alternifolium* (Wt.) Walp., Characterization and Evaluation of Antiviral Activity. *J. Clust. Sci.* **2018**, *29*, 743–755. [[CrossRef](#)]
102. Khodadadi, B.; Bordbar, M.; Yeganeh-Faal, A.; Nasrollahzadeh, M. Green Synthesis of Ag Nanoparticles/Clinoptilolite Using *Vaccinium macrocarpon* Fruit Extract and Its Excellent Catalytic Activity for Reduction of Organic Dyes. *J. Alloys Compd.* **2017**, *719*, 82–88. [[CrossRef](#)]
103. Yap, Y.H.; Azmi, A.A.; Mohd, N.K.; Yong, F.S.J.; Kan, S.Y.; Thirmizir, M.Z.A.; Chia, P.W. Green Synthesis of Silver Nanoparticle Using Water Extract of Onion Peel and Application in the Acetylation Reaction. *Arab. J. Sci. Eng.* **2020**, *45*, 4797–4807. [[CrossRef](#)]
104. Gangapuram, B.R.; Bandi, R.; Alle, M.; Dadigala, R.; Kotu, G.M.; Guttena, V. Microwave Assisted Rapid Green Synthesis of Gold Nanoparticles Using *Annona squamosa* L. Peel Extract for the Efficient Catalytic Reduction of Organic Pollutants. *J. Mol. Struct.* **2018**, *1167*, 305–315. [[CrossRef](#)]
105. Pan, Z.; Lin, Y.; Sarkar, B.; Owens, G.; Chen, Z. Green Synthesis of Iron Nanoparticles Using Red Peanut Skin Extract: Synthesis Mechanism, Characterization and Effect of Conditions on Chromium Removal. *J. Colloid Interface Sci.* **2019**, *558*, 106–114. [[CrossRef](#)] [[PubMed](#)]
106. Babita Devi, T.; Ahmaruzzaman, M. Bio-Inspired Facile and Green Synthesis of Au@Ag@AgCl Nanoparticles Using *Benincasa hispida* Peel Extract and Their Photocatalytic Activity for the Removal of Toxic Dye Under Solar Irradiation. In *Advances in Waste Management*; Kalamdhad, A.S., Singh, J., Dhamodharan, K., Eds.; Springer: Singapore, 2019; pp. 525–534. ISBN 978-981-13-0214-5.

107. Wicaksono, W.P.; Kadja, G.T.M.; Amalia, D.; Uyun, L.; Rini, W.P.; Hidayat, A.; Fahmi, R.L.; Nasriyanti, D.; Leun, S.G.V.; Ariyanta, H.A.; et al. A Green Synthesis of Gold–Palladium Core–Shell Nanoparticles Using Orange Peel Extract through Two-Step Reduction Method and Its Formaldehyde Colorimetric Sensing Performance. *Nano-Struct. Nano-Objects* **2020**, *24*, 100535. [[CrossRef](#)]
108. Yusefi, M.; Shameli, K.; Yee, O.S.; Teow, S.Y.; Hedayatnasab, Z.; Jahangirian, H.; Webster, T.J.; Kuča, K. Green Synthesis of Fe₃O₄ Nanoparticles Stabilized by a Garcinia Mangostana Fruit Peel Extract for Hyperthermia and Anticancer Activities. *Int. J. Nanomed.* **2021**, *16*, 2515–2532. [[CrossRef](#)]
109. Xin Lee, K.; Shameli, K.; Miyake, M.; Kuwano, N.; Bt Ahmad Khairudin, N.B.; Bt Mohamad, S.E.; Yew, Y.P. Green Synthesis of Gold Nanoparticles Using Aqueous Extract of *Garcinia mangostana* Fruit Peels. *J. Nanomater.* **2016**, *2016*, 8489094. [[CrossRef](#)]
110. Sasidharan, D.; Namitha, T.R.; Johnson, S.P.; Jose, V.; Mathew, P. Synthesis of Silver and Copper Oxide Nanoparticles Using *Myristica fragrans* Fruit Extract: Antimicrobial and Catalytic Applications. *Sustain. Chem. Pharm.* **2020**, *16*, 100255. [[CrossRef](#)]
111. Doan Thi, T.U.; Nguyen, T.T.; Thi, Y.D.; Ta Thi, K.H.; Phan, B.T.; Pham, K.N. Green Synthesis of ZnO Nanoparticles Using Orange Fruit Peel Extract for Antibacterial Activities. *RSC Adv.* **2020**, *10*, 23899–23907. [[CrossRef](#)]
112. Adebayo, A.E.; Oke, A.M.; Lateef, A.; Oyatokun, A.A.; Abisoye, O.D.; Adiji, I.P.; Fagbenro, D.O.; Amusan, T.V.; Badmus, J.A.; Asafa, T.B.; et al. Biosynthesis of Silver, Gold and Silver–Gold Alloy Nanoparticles Using *Persea americana* Fruit Peel Aqueous Extract for Their Biomedical Properties. *Nanotechnol. Environ. Eng.* **2019**, *4*, 13. [[CrossRef](#)]
113. Siddiqui, V.U.; Ansari, A.; Chauhan, R.; Siddiqui, W.A. Green Synthesis of Copper Oxide (CuO) Nanoparticles by Punica Granatum Peel Extract. *Mater. Today Proc.* **2019**, *36*, 751–755. [[CrossRef](#)]
114. Ghidan, A.Y.; Al-Antary, T.M.; Awwad, A.M. Green Synthesis of Copper Oxide Nanoparticles Using *Punica granatum* Peels Extract: Effect on Green Peach Aphid. *Environ. Nanotechnol. Monit. Manag.* **2016**, *6*, 95–98. [[CrossRef](#)]
115. Ravikumar, K.V.G.; Sudakaran, S.V.; Ravichandran, K.; Pulimi, M.; Natarajan, C.; Mukherjee, A. Green Synthesis of NiFe Nano Particles Using *Punica granatum* Peel Extract for Tetracycline Removal. *J. Clean. Prod.* **2019**, *210*, 767–776. [[CrossRef](#)]
116. Ehrampoush, M.H.; Miria, M.; Salmani, M.H.; Mahvi, A.H. Cadmium Removal from Aqueous Solution by Green Synthesis Iron Oxide Nanoparticles with Tangerine Peel Extract. *J. Environ. Health Sci. Eng.* **2015**, *13*, 84. [[CrossRef](#)]
117. Nava, O.J.; Soto-Robles, C.A.; Gómez-Gutiérrez, C.M.; Vilchis-Nestor, A.R.; Castro-Beltrán, A.; Olivas, A.; Luque, P.A. Fruit Peel Extract Mediated Green Synthesis of Zinc Oxide Nanoparticles. *J. Mol. Struct.* **2017**, *1147*, 43–54. [[CrossRef](#)]
118. Manjari, G.; Saran, S.; Arun, T.; Vijaya Bhaskara Rao, A.; Devipriya, S.P. Catalytic and Recyclability Properties of Phytogetic Copper Oxide Nanoparticles Derived from *Aglaia Elaeagnoides* Flower Extract. *J. Saudi Chem. Soc.* **2017**, *21*, 610–618. [[CrossRef](#)]
119. Karimi Andeani, J.; Mohsenzadeh, S. Phytosynthesis of Cadmium Oxide Nanoparticles from *Achillea Wilhelmsii* Flowers. *J. Chem.* **2013**, *2013*, 147613. [[CrossRef](#)]
120. Karimi, J.; Mohsenzadeh, S. Rapid, Green, and Eco-Friendly Biosynthesis of Copper Nanoparticles Using Flower Extract of *Aloe vera*. *Synth. React. Inorg. Met. Nano-Met. Chem.* **2015**, *45*, 895–898. [[CrossRef](#)]
121. Karpagavinayagam, P.; Vedhi, C. Green Synthesis of Iron Oxide Nanoparticles Using *Avicennia marina* Flower Extract. *Vacuum* **2019**, *160*, 286–292. [[CrossRef](#)]
122. Gopalakrishnan, V.; Muniraj, S. Neem Flower Extract Assisted Green Synthesis of Copper Nanoparticles—Optimisation, Characterisation and Anti-Bacterial Study. *Mater. Today Proc.* **2019**, *36*, 832–836. [[CrossRef](#)]
123. Elgorban, A.M.; Marraiki, N.; Ansari, S.A.; Syed, A. Green Synthesis of Cu/Fe₃O₄ nanocomposite Using *Calendula* Extract and Evaluation of Its Catalytic Activity for Chemoselective Oxidation of Sulfides to Sulfoxides with Aqueous Hydrogen Peroxide. *J. Organomet. Chem.* **2021**, *954–955*, 122077. [[CrossRef](#)]
124. Younas, U.; Gulzar, A.; Ali, F.; Pervaiz, M.; Ali, Z.; Khan, S.; Saeed, Z.; Ahmed, M.; Alothman, A.A. Antioxidant and Organic Dye Removal Potential of Cu–Ni Bimetallic Nanoparticles Synthesized Using *Gazania rigens* Extract. *Water* **2021**, *13*, 2653. [[CrossRef](#)]
125. Ghosh, S.; Patil, S.; Ahire, M.; Kitture, R.; Gurav, D.D.; Jabgunde, A.M.; Kale, S.; Pardesi, K.; Shinde, V.; Bellare, J.; et al. *Gnidia Glauca* Flower Extract Mediated Synthesis of Gold Nanoparticles and Evaluation of Its Chemocatalytic Potential. *J. Nanobiotechnol.* **2012**, *10*, 17. [[CrossRef](#)]
126. Thovhogi, N.; Diallo, A.; Gurib-Fakim, A.; Maaza, M. Nanoparticles Green Synthesis by Hibiscus Sabdariffa Flower Extract: Main Physical Properties. *J. Alloys Compd.* **2015**, *647*, 392–396. [[CrossRef](#)]
127. Patra, N.; Sahoo, A.; Behera, A. Synthesis and Differential Antibacterial Activity of Bioconjugated Bimetallic Nanoparticles. *Pharm. Chem. J.* **2020**, *54*, 865–869. [[CrossRef](#)]
128. Padalia, H.; Moteriya, P.; Chanda, S. Green Synthesis of Silver Nanoparticles from Marigold Flower and Its Synergistic Antimicrobial Potential. *Arab. J. Chem.* **2015**, *8*, 732–741. [[CrossRef](#)]
129. Dobrucka, R.; Długaszewska, J. Biosynthesis and Antibacterial Activity of ZnO Nanoparticles Using *Trifolium pratense* Flower Extract. *Saudi J. Biol. Sci.* **2016**, *23*, 517–523. [[CrossRef](#)]
130. Behravan, M.; Hossein Panahi, A.; Naghizadeh, A.; Ziaee, M.; Mahdavi, R.; Mirzapour, A. Facile Green Synthesis of Silver Nanoparticles Using *Berberis vulgaris* Leaf and Root Aqueous Extract and Its Antibacterial Activity. *Int. J. Biol. Macromol.* **2019**, *124*, 148–154. [[CrossRef](#)] [[PubMed](#)]
131. Dulta, K.; Koşarsoy Ağçeli, G.; Chauhan, P.; Jasrotia, R.; Chauhan, P.K. A Novel Approach of Synthesis Zinc Oxide Nanoparticles by *Bergenia Ciliata* Rhizome Extract: Antibacterial and Anticancer Potential. *J. Inorg. Organomet. Polym. Mater.* **2021**, *31*, 180–190. [[CrossRef](#)]

132. Nnadozie, E.C.; Ajibade, P.A. Green Synthesis and Characterization of Magnetite (Fe₃O₄) Nanoparticles Using *Chromolaena odorata* Root Extract for Smart Nanocomposite. *Mater. Lett.* **2020**, *263*, 127145. [CrossRef]
133. Wang, D.; Markus, J.; Wang, C.; Kim, Y.J.; Mathiyalagan, R.; Aceituno, V.C.; Ahn, S.; Yang, D.C. Green Synthesis of Gold and Silver Nanoparticles Using Aqueous Extract of *Cibotium barometz* Root. *Artif. Cells Nanomed. Biotechnol.* **2017**, *45*, 1548–1555. [CrossRef]
134. Rao, N.H.; Lakshmidevi, N.; Pammi, S.V.N.; Kollu, P.; Ganapaty, S.; Lakshmi, P. Green Synthesis of Silver Nanoparticles Using Methanolic Root Extracts of *Diospyros paniculata* and Their Antimicrobial Activities. *Mater. Sci. Eng. C* **2016**, *62*, 553–557. [CrossRef]
135. Al-Radadi, N.S. Facile One-Step Green Synthesis of Gold Nanoparticles (AuNp) Using Licorice Root Extract: Antimicrobial and Anticancer Study against HepG2 Cell Line. *Arab. J. Chem.* **2021**, *14*, 102956. [CrossRef]
136. Suman, T.Y.; Radhika Rajasree, S.R.; Ramkumar, R.; Rajthilak, C.; Perumal, P. The Green Synthesis of Gold Nanoparticles Using an Aqueous Root Extract of *Morinda citrifolia* L. *Spectrochim. Acta Part A Mol. Biomol. Spectrosc.* **2014**, *118*, 11–16. [CrossRef]
137. Singh, J.; Dhaliwal, A.S. Novel Green Synthesis and Characterization of the Antioxidant Activity of Silver Nanoparticles Prepared from *Nepeta leucophylla* Root Extract. *Anal. Lett.* **2019**, *52*, 213–230. [CrossRef]
138. Singh, P.; Kim, Y.J.; Wang, C.; Mathiyalagan, R.; Yang, D.C. The Development of a Green Approach for the Biosynthesis of Silver and Gold Nanoparticles by Using *Panax ginseng* Root Extract, and Their Biological Applications. *Artif. Cells Nanomed. Biotechnol.* **2016**, *44*, 1150–1157. [CrossRef]
139. Bordbar, M.; Sharifi-Zarchi, Z.; Khodadadi, B. Green Synthesis of Copper Oxide Nanoparticles/Clinoptilolite Using *Rheum palmatum* L. Root Extract: High Catalytic Activity for Reduction of 4-Nitro Phenol, Rhodamine B, and Methylene Blue. *J. Sol-Gel Sci. Technol.* **2017**, *81*, 724–733. [CrossRef]
140. Arokiyaraj, S.; Vincent, S.; Saravanan, M.; Lee, Y.; Oh, Y.K.; Kim, K.H. Green Synthesis of Silver Nanoparticles Using *Rheum palmatum* Root Extract and Their Antibacterial Activity against *Staphylococcus Aureus* and *Pseudomonas Aeruginosa*. *Artif. Cells Nanomed. Biotechnol.* **2017**, *45*, 372–379. [CrossRef]
141. Hu, D.; Yang, X.; Chen, W.; Feng, Z.; Hu, C.; Yan, F.; Chen, X.; Qu, D.; Chen, Z. Rhodiola Rosea Rhizome Extract-Mediated Green Synthesis of Silver Nanoparticles and Evaluation of Their Potential Antioxidant and Catalytic Reduction Activities. *ACS Omega* **2021**, *6*, 24450–24461. [CrossRef] [PubMed]
142. Chen, L.; Batjikh, I.; Hurh, J.; Han, Y.; Huo, Y.; Ali, H.; Li, J.F.; Rupa, E.J.; Ahn, J.C.; Mathiyalagan, R.; et al. Green Synthesis of Zinc Oxide Nanoparticles from Root Extract of *Scutellaria baicalensis* and Its Photocatalytic Degradation Activity Using Methylene Blue. *Optik* **2019**, *184*, 324–329. [CrossRef]
143. Judith Vijaya, J.; Jayaprakash, N.; Kombaiah, K.; Kaviyarasu, K.; John Kennedy, L.; Jothi Ramalingam, R.; Al-Lohedan, H.A.; Mansoor-Ali, V.M.; Maaza, M. Bioreduction Potentials of Dried Root of Zingiber Officinale for a Simple Green Synthesis of Silver Nanoparticles: Antibacterial Studies. *J. Photochem. Photobiol. B Biol.* **2017**, *177*, 62–68. [CrossRef] [PubMed]
144. Velmurugan, P.; Anbalagan, K.; Manosathyadevan, M.; Lee, K.J.; Cho, M.; Lee, S.M.; Park, J.H.; Oh, S.G.; Bang, K.S.; Oh, B.T. Green Synthesis of Silver and Gold Nanoparticles Using *Zingiber officinale* Root Extract and Antibacterial Activity of Silver Nanoparticles against Food Pathogens. *Bioprocess Biosyst. Eng.* **2014**, *37*, 1935–1943. [CrossRef]
145. Maurya, I.C.; Singh, S.; Senapati, S.; Srivastava, P.; Bahadur, L. Green Synthesis of TiO₂ Nanoparticles Using *Bixa orellana* Seed Extract and Its Application for Solar Cells. *Sol. Energy* **2019**, *194*, 952–958. [CrossRef]
146. Sukumar, S.; Rudrasenan, A.; Padmanabhan Nambiar, D. Green-Synthesized Rice-Shaped Copper Oxide Nanoparticles Using *Caesalpinia bonducella* Seed Extract and Their Applications. *ACS Omega* **2020**, *5*, 1040–1051. [CrossRef]
147. Bogireddy, N.K.R.; Pal, U.; Gomez, L.M.; Agarwal, V. Size Controlled Green Synthesis of Gold Nanoparticles Using *Coffea arabica* Seed Extract and Their Catalytic Performance in 4-Nitrophenol Reduction. *RSC Adv.* **2018**, *8*, 24819–24826. [CrossRef]
148. Abisharani, J.M.; Devikala, S.; Dinesh Kumar, R.; Arthanareeswari, M.; Kamaraj, P. Green Synthesis of TiO₂ Nanoparticles Using *Cucurbita pepo* Seeds Extract. *Mater. Today Proc.* **2019**, *14*, 302–307. [CrossRef]
149. Shabaani, M.; Rahaiee, S.; Zare, M.; Jafari, S.M. Green Synthesis of ZnO Nanoparticles Using Loquat Seed Extract; Biological Functions and Photocatalytic Degradation Properties. *LWT* **2020**, *134*, 110133. [CrossRef]
150. Girón-Vázquez, N.G.; Gómez-Gutiérrez, C.M.; Soto-Robles, C.A.; Nava, O.; Lugo-Medina, E.; Castrejón-Sánchez, V.H.; Vilchis-Nestor, A.R.; Luque, P.A. Study of the Effect of Persea Americana Seed in the Green Synthesis of Silver Nanoparticles and Their Antimicrobial Properties. *Results Phys.* **2019**, *13*, 102142. [CrossRef]
151. Ansari, M.A.; Alzohairy, M.A. One-Pot Facile Green Synthesis of Silver Nanoparticles Using Seed Extract of *Phoenix dactylifera* and Their Bactericidal Potential against MRSA. *Evid. Based Complement. Altern. Med.* **2018**, *2018*, 4923062. [CrossRef] [PubMed]
152. Qidwai, A.; Kumar, R.; Dikshit, A. Green Synthesis of Silver Nanoparticles by Seed of *Phoenix sylvestris* L. and Their Role in the Management of Cosmetics Embarrassment. *Green Chem. Lett. Rev.* **2018**, *11*, 176–188. [CrossRef]
153. Meena Kumari, M.; Jacob, J.; Philip, D. Green Synthesis and Applications of Au-Ag Bimetallic Nanoparticles. *Spectrochim. Acta Part A Mol. Biomol. Spectrosc.* **2015**, *137*, 185–192. [CrossRef] [PubMed]
154. Nazar, N.; Bibi, I.; Kamal, S.; Iqbal, M.; Nouren, S.; Jilani, K.; Umair, M.; Ata, S. Cu Nanoparticles Synthesis Using Biological Molecule of *P. granatum* Seeds Extract as Reducing and Capping Agent: Growth Mechanism and Photo-Catalytic Activity. *Int. J. Biol. Macromol.* **2018**, *106*, 1203–1210. [CrossRef]
155. Bibi, I.; Nazar, N.; Ata, S.; Sultan, M.; Ali, A.; Abbas, A.; Jilani, K.; Kamal, S.; Sarim, F.M.; Khan, M.I.; et al. Green Synthesis of Iron Oxide Nanoparticles Using Pomegranate Seeds Extract and Photocatalytic Activity Evaluation for the Degradation of Textile Dye. *J. Mater. Res. Technol.* **2019**, *8*, 6115–6124. [CrossRef]

156. Tabrizi Hafez Moghaddas, S.M.; Elahi, B.; Javanbakht, V. Biosynthesis of Pure Zinc Oxide Nanoparticles Using Quince Seed Mucilage for Photocatalytic Dye Degradation. *J. Alloys Compd.* **2020**, *821*, 153519. [[CrossRef](#)]
157. Sabouri, Z.; Rangrazi, A.; Amiri, M.S.; Khatami, M.; Darroudi, M. Green Synthesis of Nickel Oxide Nanoparticles Using *Salvia hispanica* L. (Chia) Seeds Extract and Studies of Their Photocatalytic Activity and Cytotoxicity Effects. *Bioprocess Biosyst. Eng.* **2021**, *44*, 2407–2415. [[CrossRef](#)]
158. Rautela, A.; Rani, J.; Debnath (Das), M. Green Synthesis of Silver Nanoparticles from *Tectona Grandis* Seeds Extract: Characterization and Mechanism of Antimicrobial Action on Different Microorganisms. *J. Anal. Sci. Technol.* **2019**, *10*, 5. [[CrossRef](#)]
159. Yulizar, Y.; Bakri, R.; Apriandanu, D.O.B.; Hidayat, T. ZnO/CuO Nanocomposite Prepared in One-Pot Green Synthesis Using Seed Bark Extract of *Theobroma cacao*. *Nano-Struct. Nano-Objects* **2018**, *16*, 300–305. [[CrossRef](#)]
160. Babu, A.K.; Kumaresan, G.; Raj, V.A.A.; Velraj, R. Review of Leaf Drying: Mechanism and Influencing Parameters, Drying Methods, Nutrient Preservation, and Mathematical Models. *Renew. Sustain. Energy Rev.* **2018**, *90*, 536–556. [[CrossRef](#)]
161. Sridhar, A.; Ponnuchamy, M.; Kumar, P.S.; Kapoor, A.; Vo, D.-V.N.; Prabhakar, S. Techniques and Modeling of Polyphenol Extraction from Food: A Review. *Environ. Chem. Lett.* **2021**, *19*, 3409–3443. [[CrossRef](#)] [[PubMed](#)]
162. Wang, L.; Weller, C.L. Recent Advances in Extraction of Nutraceuticals from Plants. *Trends Food Sci. Technol.* **2006**, *17*, 300–312. [[CrossRef](#)]
163. Bozinou, E.; Karageorgou, I.; Batra, G.; Dourtoglou, V.G.; Lalas, S.I. Pulsed Electric Field Extraction and Antioxidant Activity Determination of *Moringa oleifera* Dry Leaves: A Comparative Study with Other Extraction Techniques. *Beverages* **2019**, *5*, 8. [[CrossRef](#)]
164. Che Sulaiman, I.S.; Basri, M.; Fard Masoumi, H.R.; Chee, W.J.; Ashari, S.E.; Ismail, M. Effects of Temperature, Time, and Solvent Ratio on the Extraction of Phenolic Compounds and the Anti-Radical Activity of *Clinacanthus Nutans* Lindau Leaves by Response Surface Methodology. *Chem. Cent. J.* **2017**, *11*, 54. [[CrossRef](#)] [[PubMed](#)]
165. Do, Q.D.; Angkawijaya, A.E.; Tran-Nguyen, P.L.; Huynh, L.H.; Soetaredjo, F.E.; Ismadji, S.; Ju, Y.-H. Effect of Extraction Solvent on Total Phenol Content, Total Flavonoid Content, and Antioxidant Activity of *Limnophila aromatica*. *J. Food Drug Anal.* **2014**, *22*, 296–302. [[CrossRef](#)]
166. Lapornik, B.; Prošek, M.; Golc Wondra, A. Comparison of Extracts Prepared from Plant By-Products Using Different Solvents and Extraction Time. *J. Food Eng.* **2005**, *71*, 214–222. [[CrossRef](#)]
167. Vanlalveni, C.; Lallianrawna, S.; Biswas, A.; Selvaraj, M.; Changmai, B.; Rokhum, S.L. Green Synthesis of Silver Nanoparticles Using Plant Extracts and Their Antimicrobial Activities: A Review of Recent Literature. *RSC Adv.* **2021**, *11*, 2804–2837. [[CrossRef](#)]
168. Laorko, A.; Tongchitpakdee, S.; Youravong, W. Storage Quality of Pineapple Juice Non-Thermally Pasteurized and Clarified by Microfiltration. *J. Food Eng.* **2013**, *116*, 554–561. [[CrossRef](#)]
169. Issaabadi, Z.; Nasrollahzadeh, M.; Sajadi, S.M. Green Synthesis of the Copper Nanoparticles Supported on Bentonite and Investigation of Its Catalytic Activity. *J. Clean. Prod.* **2017**, *142*, 3584–3591. [[CrossRef](#)]
170. Dobrucka, R.; Dlugaszewska, J. Antimicrobial Activity of the Biogenically Synthesized Core-Shell Cu@Pt Nanoparticles. *Saudi Pharm. J.* **2018**, *26*, 643–650. [[CrossRef](#)] [[PubMed](#)]
171. Rajendaran, K.; Muthuramalingam, R.; Ayyadurai, S. Green Synthesis of Ag-Mo/CuO Nanoparticles Using *Azadirachta indica* Leaf Extracts to Study Its Solar Photocatalytic and Antimicrobial Activities. *Mater. Sci. Semicond. Process.* **2019**, *91*, 230–238. [[CrossRef](#)]
172. Rosbero, T.M.S.; Camacho, D.H. Green Preparation and Characterization of Tentacle-like Silver/Copper Nanoparticles for Catalytic Degradation of Toxic Chlorpyrifos in Water. *J. Environ. Chem. Eng.* **2017**, *5*, 2524–2532. [[CrossRef](#)]
173. Suvarna, A.R.; Shetty, A.; Anchan, S.; Kabeer, N.; Nayak, S. Cyclea Peltata Leaf Mediated Green Synthesized Bimetallic Nanoparticles Exhibits Methyl Green Dye Degradation Capability. *Bionanoscience* **2020**, *10*, 606–617. [[CrossRef](#)]
174. Dayakar, T.; Venkateswara Rao, K.; Park, J.; Krishna, P.; Swaroopa, P.; Ji, Y. Biosynthesis of Ag@CuO Core-Shell Nanostructures for Non-Enzymatic Glucose Sensing Using Screen-Printed Electrode. *J. Mater. Sci. Mater. Electron.* **2019**, *30*, 9725–9734. [[CrossRef](#)]
175. Rocha-Rocha, O.; Cortez-Valadez, M.; Hernández-Martínez, A.R.; Gámez-Corrales, R.; Alvarez, R.A.B.; Britto-Hurtado, R.; Delgado-Beleño, Y.; Martínez-Nuñez, C.E.; Pérez-Rodríguez, A.; Arizpe-Chávez, H.; et al. Green Synthesis of Ag-Cu Nanoalloys Using *Opuntia ficus-indica*. *J. Electron. Mater.* **2017**, *46*, 802–807. [[CrossRef](#)]
176. Alshehri, A.A.; Malik, M.A. Facile One-Pot Biogenic Synthesis of Cu-Co-Ni Trimetallic Nanoparticles for Enhanced Photocatalytic Dye Degradation. *Catalysts* **2020**, *10*, 1138. [[CrossRef](#)]
177. Suresh, J.; Ragunath, L.; Hong, S.I. Biosynthesis of Mixed Nanocrystalline Zn-Mg-Cu Oxide Nanocomposites and Their Antimicrobial Behavior. *Adv. Nat. Sci. Nanosci. Nanotechnol.* **2019**, *10*, 045014. [[CrossRef](#)]
178. Mamatha, G.; Sowmya, P.; Madhuri, D.; Mohan Babu, N.; Suresh Kumar, D.; Vijaya Charan, G.; Varaprasad, K.; Madhukar, K. Antimicrobial Cellulose Nanocomposite Films with In Situ Generations of Bimetallic (Ag and Cu) Nanoparticles Using *Vitex negundo* Leaves Extract. *J. Inorg. Organomet. Polym. Mater.* **2021**, *31*, 802–815. [[CrossRef](#)]
179. Amaliyah, S.; Pangesti, D.P.; Masruri, M.; Sabarudin, A.; Sumitro, S.B. Green Synthesis and Characterization of Copper Nanoparticles Using *Piper retrofractum* Vahl Extract as Bioreductor and Capping Agent. *Heliyon* **2020**, *6*, e04636. [[CrossRef](#)]
180. Biresaw, S.S.; Taneja, P. Copper Nanoparticles Green Synthesis and Characterization as Anticancer Potential in Breast Cancer Cells (MCF7) Derived from *Prunus Nepalensis* Phytochemicals. *Mater. Today Proc.* **2022**, *49*, 3501–3509. [[CrossRef](#)]
181. Hemmati, S.; Mehrazin, L.; Hekmati, M.; Izadi, M.; Veisi, H. Biosynthesis of CuO Nanoparticles Using *Rosa canina* Fruit Extract as a Recyclable and Heterogeneous Nanocatalyst for C-N Ullmann Coupling Reactions. *Mater. Chem. Phys.* **2018**, *214*, 527–532. [[CrossRef](#)]

182. Kumar, B.; Smita, K.; Cumbal, L.; Debut, A.; Angulo, Y. Biofabrication of Copper Oxide Nanoparticles Using Andean Blackberry (*Rubus glaucus* Benth.) Fruit and Leaf. *J. Saudi Chem. Soc.* **2017**, *21*, S475–S480. [[CrossRef](#)]
183. Khani, R.; Roostaei, B.; Bagherzade, G.; Moudi, M. Green Synthesis of Copper Nanoparticles by Fruit Extract of *Ziziphus spinachristi* (L.) Willd.: Application for Adsorption of Triphenylmethane Dye and Antibacterial Assay. *J. Mol. Liq.* **2018**, *255*, 541–549. [[CrossRef](#)]
184. Aminuzzaman, M.; Kei, L.M.; Liang, W.H. Green Synthesis of Copper Oxide (CuO) Nanoparticles Using Banana Peel Extract and Their Photocatalytic Activities. In *AIP Conference Proceedings*; AIP Publishing LLC: New York, NY, USA, 2017; Volume 1828. [[CrossRef](#)]
185. Ghaffar, A.; Kiran, S.; Rafique, M.A.; Iqbal, S.; Nosheen, S.; Hou, Y.; Afzal, G.; Bashir, M.; Aimun, U. Citrus Paradisi Fruit Peel Extract Mediated Green Synthesis of Copper Nanoparticles for Remediation of Disperse Yellow 125 Dye. *Desalin. Water Treat.* **2021**, *212*, 368–375. [[CrossRef](#)]
186. Ituen, E.; Ekemini, E.; Yuanhua, L.; Li, R.; Singh, A. Mitigation of Microbial Biodeterioration and Acid Corrosion of Pipework Steel Using *Citrus reticulata* Peels Extract Mediated Copper Nanoparticles Composite. *Int. Biodeterior. Biodegrad.* **2020**, *149*, 104935. [[CrossRef](#)]
187. Kaur, P.; Thakur, R.; Chaudhury, A. Biogenesis of Copper Nanoparticles Using Peel Extract of *Punica granatum* and Their Antimicrobial Activity against Opportunistic Pathogens. *Green Chem. Lett. Rev.* **2016**, *9*, 33–38. [[CrossRef](#)]
188. Manjari, G.; Saran, S.; Radhakrishanan, S.; Rameshkumar, P.; Pandikumar, A.; Devipriya, S.P. Facile Green Synthesis of Ag–Cu Decorated ZnO Nanocomposite for Effective Removal of Toxic Organic Compounds and an Efficient Detection of Nitrite Ions. *J. Environ. Manag.* **2020**, *262*, 110282. [[CrossRef](#)]
189. Roy, K.; Ghosh, C.K.; Sarkar, C.K. Rapid Detection of Hazardous H₂O₂ by Biogenic Copper Nanoparticles Synthesized Using *Eichhornia crassipes* Extract. *Microsyst. Technol.* **2019**, *25*, 1699–1703. [[CrossRef](#)]
190. Chowdhury, R.; Khan, A.; Rashid, M.H. Green Synthesis of CuO Nanoparticles Using *Lantana camara* Flower Extract and Their Potential Catalytic Activity towards the Aza-Michael Reaction. *RSC Adv.* **2020**, *10*, 14374–14385. [[CrossRef](#)]
191. Thakur, S.; Sharma, S.; Thakur, S.; Rai, R. Green Synthesis of Copper Nano-Particles Using *Asparagus adscendens* Roxb. Root and Leaf Extract and Their Antimicrobial Activities. *Int. J. Curr. Microbiol. Appl. Sci.* **2018**, *7*, 683–694. [[CrossRef](#)]
192. Pallela, P.N.V.K.; Ummey, S.; Ruddaraju, L.K.; Kollu, P.; Khan, S.; Pammi, S.V.N. Antibacterial Activity Assessment and Characterization of Green Synthesized CuO Nano Rods Using *Asparagus racemosus* Roots Extract. *SN Appl. Sci.* **2019**, *1*, 421. [[CrossRef](#)]
193. Selvam, K.; Sudhakar, C.; Selvankumar, T.; Senthilkumar, B.; Selva Kumar, R.; Kannan, N. Biomimetic Synthesis of Copper Nanoparticles Using Rhizome Extract of *Corallocarbus epigaeus* and Their Bactericidal with Photocatalytic Activity. *SN Appl. Sci.* **2020**, *2*, 1028. [[CrossRef](#)]
194. Maulana, I.; Fasya, D.; Ginting, B. Biosynthesis of Cu Nanoparticles Using *Polyalthia longifolia* Roots Extracts for Antibacterial, Antioxidant and Cytotoxicity Applications. *Mater. Technol.* **2022**, 1–5. [[CrossRef](#)]
195. Sharma, D.; Ledwani, L.; Kumar, N.; Mehrotra, T.; Pervaiz, N.; Kumar, R. An Investigation of Physicochemical and Biological Properties of Rheum Emodi-Mediated Bimetallic Ag–Cu Nanoparticles. *Arab. J. Sci. Eng.* **2021**, *46*, 275–285. [[CrossRef](#)]
196. Sadia, B.O.; Cherutoi, J.K.; Achisa, C.M. Optimization, Characterization, and Antibacterial Activity of Copper Nanoparticles Synthesized Using *Senna didymobotrya* Root Extract. *J. Nanotechnol.* **2021**, *2021*, 1–15. [[CrossRef](#)]
197. Varghese, B.; Kurian, M.; Krishna, S.; Athira, T.S. Biochemical Synthesis of Copper Nanoparticles Using *Zingiber officinalis* and Curcuma Longa: Characterization and Antibacterial Activity Study. *Mater. Today Proc.* **2019**, *25*, 302–306. [[CrossRef](#)]
198. Heydari, R.; Koudehi, M.F.; Pourmortazavi, S.M. Antibacterial Activity of Fe₃O₄/Cu Nanocomposite: Green Synthesis Using *Carum carvi* L. Seeds Aqueous Extract. *ChemistrySelect* **2019**, *4*, 531–535. [[CrossRef](#)]
199. Jasrotia, T.; Chaudhary, S.; Kaushik, A.; Kumar, R.; Chaudhary, G.R. Green Chemistry-Assisted Synthesis of Biocompatible Ag, Cu, and Fe₂O₃ Nanoparticles. *Mater. Today Chem.* **2020**, *15*, 100214. [[CrossRef](#)]
200. Rajeshkumar, S.; Rinitha, G. Nanostructural Characterization of Antimicrobial and Antioxidant Copper Nanoparticles Synthesized Using *Novel persea Americana* Seeds. *OpenNano* **2018**, *3*, 18–27. [[CrossRef](#)]
201. Sajadi, S.M.; Nasrollahzadeh, M.; Maham, M. Aqueous Extract from Seeds of *Silybum marianum* L. as a Green Material for Preparation of the Cu/Fe₃O₄ Nanoparticles: A Magnetically Recoverable and Reusable Catalyst for the Reduction of Nitroarenes. *J. Colloid Interface Sci.* **2016**, *469*, 93–98. [[CrossRef](#)] [[PubMed](#)]
202. Nasrollahzadeh, M.; Sajadi, S.M.; Rostami-Vartooni, A.; Bagherzadeh, M. Green Synthesis of Pd/CuO Nanoparticles by *Theobroma cacao* L. Seeds Extract and Their Catalytic Performance for the Reduction of 4-Nitrophenol and Phosphine-Free Heck Coupling Reaction under Aerobic Conditions. *J. Colloid Interface Sci.* **2015**, *448*, 106–113. [[CrossRef](#)] [[PubMed](#)]
203. Buazar, F.; Sweidi, S.; Badri, M.; Kroushawi, F. Biofabrication of Highly Pure Copper Oxide Nanoparticles Using Wheat Seed Extract and Their Catalytic Activity: A Mechanistic Approach. *Green Process. Synth.* **2019**, *8*, 691–702. [[CrossRef](#)]
204. Singh, P.; Singh, K.R.; Singh, J.; Das, S.N.; Singh, R.P. Tunable Electrochemistry and Efficient Antibacterial Activity of Plant-Mediated Copper Oxide Nanoparticles Synthesized by *Annona squamosa* Seed Extract for Agricultural Utility. *RSC Adv.* **2021**, *11*, 18050–18060. [[CrossRef](#)] [[PubMed](#)]
205. Letchumanan, D.; Sok, S.P.M.; Ibrahim, S.; Nagoor, N.H.; Arshad, N.M. Plant-Based Biosynthesis of Copper/Copper Oxide Nanoparticles: An Update on Their Applications in Biomedicine, Mechanisms, and Toxicity. *Biomolecules* **2021**, *11*, 564. [[CrossRef](#)]

206. Bhavyasree, P.G.; Xavier, T.S. Green Synthesised Copper and Copper Oxide Based Nanomaterials Using Plant Extracts and Their Application in Antimicrobial Activity: Review. *Curr. Res. Green Sustain. Chem.* **2022**, *5*, 100249. [[CrossRef](#)]
207. Akintelu, S.A.; Folorunso, A.S.; Folorunso, F.A.; Oyebamiji, A.K. Green Synthesis of Copper Oxide Nanoparticles for Biomedical Application and Environmental Remediation. *Heliyon* **2020**, *6*, e04508. [[CrossRef](#)]
208. Klinger, M.; Theiler, M.; Bosshard, P.P. Epidemiological and Clinical Aspects of Trichophyton Mentagrophytes/Trichophyton Interdigitale Infections in the Zurich Area: A Retrospective Study Using Genotyping. *J. Eur. Acad. Dermatol. Venereol.* **2021**, *35*, 1017–1025. [[CrossRef](#)]
209. D'Enfert, C.; Kaune, A.-K.; Alaban, L.-R.; Chakraborty, S.; Cole, N.; Delavy, M.; Kosmala, D.; Marsaux, B.; Fróis-Martins, R.; Morelli, M.; et al. The Impact of the Fungus-Host-Microbiota Interplay upon *Candida albicans* Infections: Current Knowledge and New Perspectives. *FEMS Microbiol. Rev.* **2021**, *45*, fuaa060. [[CrossRef](#)]
210. Mali, S.C.; Dhaka, A.; Githala, C.K.; Trivedi, R. Green Synthesis of Copper Nanoparticles Using *Celastrus paniculatus* Willd. Leaf Extract and Their Photocatalytic and Antifungal Properties. *Biotechnol. Rep.* **2020**, *27*, e00518. [[CrossRef](#)] [[PubMed](#)]
211. Rehana, D.; Mahendiran, D.; Kumar, R.S.; Rahiman, A.K. Evaluation of Antioxidant and Anticancer Activity of Copper Oxide Nanoparticles Synthesized Using Medicinally Important Plant Extracts. *Biomed. Pharmacother.* **2017**, *89*, 1067–1077. [[CrossRef](#)] [[PubMed](#)]
212. Gawande, M.B.; Goswami, A.; Felpin, F.-X.; Asefa, T.; Huang, X.; Silva, R.; Zou, X.; Zboril, R.; Varma, R.S. Cu and Cu-Based Nanoparticles: Synthesis and Applications in Catalysis. *Chem. Rev.* **2016**, *116*, 3722–3811. [[CrossRef](#)] [[PubMed](#)]
213. Wu, S.; Ni, Z.; Wang, R.; Zhao, B.; Han, Y.; Zheng, Y.; Liu, F.; Gong, Y.; Tang, F.; Liu, Y. The Effects of Cultivar and Climate Zone on Phytochemical Components of Walnut (*Juglans regia* L.). *Food Energy Secur.* **2020**, *9*, e196. [[CrossRef](#)]
214. Szakiel, A.; Paćzkowski, C.; Henry, M. Influence of Environmental Abiotic Factors on the Content of Saponins in Plants. *Phytochem. Rev.* **2011**, *10*, 471–491. [[CrossRef](#)]
215. Park, Y.D.; Lee, Y.M.; Kang, M.A.; Lee, H.J.; Jin, C.H.; Choi, D.S.; Kim, D.S.; Kang, S.Y.; Kim, W.G.; Jeong, I.Y. Phytochemical Profiles and in Vitro Anti-Inflammatory Properties of Perilla Frutescens Cv. Chookyoupjaso Mutants Induced by Mutagenesis with γ -Ray. *Food Sci. Biotechnol.* **2010**, *19*, 305–311. [[CrossRef](#)]
216. Nielsen, E.; Temporiti, M.E.E.; Cella, R. Improvement of Phytochemical Production by Plant Cells and Organ Culture and by Genetic Engineering. *Plant Cell Rep.* **2019**, *38*, 1199–1215. [[CrossRef](#)]
217. Nagajyothi, P.C.; Muthuraman, P.; Sreekanth, T.V.M.; Kim, D.H.; Shim, J. Green Synthesis: In-Vitro Anticancer Activity of Copper Oxide Nanoparticles against Human Cervical Carcinoma Cells. *Arab. J. Chem.* **2017**, *10*, 215–225. [[CrossRef](#)]
218. Panneerselvam, C.; Murugan, K.; Roni, M.; Aziz, A.T.; Suresh, U.; Rajaganesh, R.; Madhiyazhagan, P.; Subramaniam, J.; Dinesh, D.; Nicoletti, M.; et al. Fern-Synthesized Nanoparticles in the Fight against Malaria: LC/MS Analysis of *Pteridium aquilinum* Leaf Extract and Biosynthesis of Silver Nanoparticles with High Mosquitocidal and Antiplasmodial Activity. *Parasitol. Res.* **2016**, *115*, 997–1013. [[CrossRef](#)]
219. De Araujo, A.R.; Ramos-Jesus, J.; de Oliveira, T.M.; de Carvalho, A.M.A.; Nunes, P.H.M.; Daboit, T.C.; Carvalho, A.P.; Barroso, M.F.; de Almeida, M.P.; Plácido, A.; et al. Identification of Eschweilenol C in Derivative of *Terminalia fagifolia* Mart. and Green Synthesis of Bioactive and Biocompatible Silver Nanoparticles. *Ind. Crops Prod.* **2019**, *137*, 52–65. [[CrossRef](#)]
220. Tao, H.; Wu, T.; Aldeghi, M.; Wu, T.C.; Aspuru-Guzik, A.; Kumacheva, E. Nanoparticle Synthesis Assisted by Machine Learning. *Nat. Rev. Mater.* **2021**, *6*, 701–716. [[CrossRef](#)]
221. Lv, H.; Chen, X. Intelligent Control of Nanoparticle Synthesis through Machine Learning. *Nanoscale* **2022**, *14*, 6688–6708. [[CrossRef](#)] [[PubMed](#)]
222. Mekki-Berrada, F.; Ren, Z.; Huang, T.; Wong, W.K.; Zheng, F.; Xie, J.; Tian, I.P.S.; Jayavelu, S.; Mahfoud, Z.; Bash, D.; et al. Two-Step Machine Learning Enables Optimized Nanoparticle Synthesis. *NPJ Comput. Mater.* **2021**, *7*, 55. [[CrossRef](#)]
223. Devaraj, T.; Aathika, S.; Mani, Y.; Jagadiswary, D.; Evangeline, S.J.; Dhanasekaran, A.; Palaniyandi, S.; Subramanian, S. Application of Artificial Neural Network as a Nonhazardous Alternative on Kinetic Analysis and Modeling for Green Synthesis of Cobalt Nanocatalyst from *Ocimum tenuiflorum*. *J. Hazard. Mater.* **2021**, *416*, 125720. [[CrossRef](#)] [[PubMed](#)]
224. Pellegrino, F.; Isopescu, R.; Pellutiè, L.; Sordello, F.; Rossi, A.M.; Ortel, E.; Martra, G.; Hodoroaba, V.-D.; Maurino, V. Machine Learning Approach for Elucidating and Predicting the Role of Synthesis Parameters on the Shape and Size of TiO₂ Nanoparticles. *Sci. Rep.* **2020**, *10*, 18910. [[CrossRef](#)]